ACADÉMIE
DES SCIENCES
INSTITUT DE FRANCE

Comptes Rendus
Chimie

Madani Hedidi, William Erb, Sirine Boussandel, Yury Siarheevich Halauko, Vadim Edvardovich Matulis, Jean-Pierre Hurvois, Marielle Blot, Thierry Roisnel, Ali Samarat and Florence Mongin

From deprotometalation of ferrocenyl ketones to fused ferrocene structures

Volume 29 (2026), p. 27-51

Online since: 22 January 2026

https://doi.org/10.5802/crchim.429

This article is licensed under the
Creative Commons Attribution 4.0 International License.
http://creativecommons.org/licenses/by/4.0/

The Comptes Rendus. Chimie *are a member of the Mersenne Center for open scientific publishing*
www.centre-mersenne.org — e-ISSN : 1878-1543

ACADÉMIE DES SCIENCES
INSTITUT DE FRANCE

Comptes Rendus. Chimie
2026, Vol. 29, p. 27-51
https://doi.org/10.5802/crchim.429

Research article

From deprotometalation of ferrocenyl ketones to fused ferrocene structures

Madani Hedidi [a,b], William Erb [*,a], Sirine Boussandel [a,c], Yury Siarheevich Halauko [*,d], Vadim Edvardovich Matulis [d], Jean-Pierre Hurvois [a], Marielle Blot [a], Thierry Roisnel [a], Ali Samarat [c] and Florence Mongin [*,a]

[a] Univ Rennes, CNRS, ISCR (Institut des Sciences Chimiques de Rennes) – UMR 6226, F-35000 Rennes, France

[b] Laboratoire de Chimie des Matériaux, Catalyse et Réactivité, Département de Chimie, Faculté des Sciences Exactes et d'Informatique, Université Hassiba Benbouali de Chlef, Ouled Fares Chlef, BP 78C, 02180 Chlef, Algérie

[c] University of Carthage, Faculty of Sciences of Bizerte, Laboratory of Hetero-Organic Compounds and Nanostructured Materials (LR18ES11), Zarzouna, 7021 Bizerte, Tunisia

[d] Department of Chemistry, Belarusian State University, 14 Leningradskaya St., 220030 Minsk, Belarus

E-mails: william.erb@univ-rennes.fr (W. Erb), hys@tut.by (Y. S. Halauko), florence.mongin@univ-rennes.fr (F. Mongin)

Abstract. Although ferrocene ketones have been known since the early days of ferrocene chemistry, their behavior in deprotometalation has never been studied in detail. Here, we have optimized this reaction using lithium 2,2,6,6-tetramethylpiperidide in tetrahydrofuran containing $ZnCl_2$·*N*,*N*,*N*′,*N*′-tetramethylethylenediamine as an in-situ trap. Numerous 2-iodoferrocene derivatives were obtained, while a change in regioselectivity was observed for certain aroyl- and heteroaroylferrocenes, in good agreement with our DFT calculations. The development of an enantioselective deprotometalation was also attempted using lithium di[(*S*)-1-phenylethyl]amide, affording the desired compounds in up to 60% enantiomeric excess (*ee*). A selection of iodinated derivatives was finally subjected to post-functionalizations, leading to original ferrocene-fused heterocycles, including an enantiopure tetracyclic derivative. A selection of compounds was studied in both electrochemical reduction and oxidation, and weak interactions such as halogen–halogen, halogen–oxygen and chalcogen–chalcogen bonds were identified in the solid state for some new derivatives.

Keywords. Ferrocene, Ketone, Deprotometalation, Selectivity, Polycyclic compounds.

Funding. Algerian Direction Générale de la Recherche Scientifique et du Développement Technologique, Rennes Métropole, University of Carthage, Tunisian Ministry of Higher Education and Scientific Research, Fonds Européen de Développement Régional, Université de Rennes, Centre National de la Recherche Scientifique, BASF, Thermofisher.

Note. Article submitted by invitation.

Manuscript received 22 September 2025, revised 17 October 2025, accepted 20 October 2025, online since 22 January 2026.

[*] Corresponding authors

1. Introduction

Since the discovery and the structure determination of the parent molecule [1–4], ferrocenes have attracted considerable interest from synthetic chemists due to their numerous applications [5–13], such as catalysis [14–17], materials science [18,19], molecular sensing [20,21], and bioorganometallic chemistry [22–25]. In addition to monosubstituted ferrocenes, which can be synthesized from ferrocene via aromatic electrophilic substitution [26] or deprotometalation/trapping sequences [27,28], polysubstituted structures may be required for targeted applications [29–33]. Among the most commonly used motifs, 1,1′-disubstituted derivatives are often obtained by double deprotolithiation of ferrocene [34], while 1,2-disubstituted derivatives are typically prepared by directed functionalization of monosubstituted ferrocenes [35–38].

As a bulky electron-rich aromatic, ferrocene tends to reduce the electrophilicity of the attached functional group [39,40]. However, although ferrocene ketones are readily accessible by Friedel–Crafts acylation of ferrocene [41], exploiting this change in reactivity to promote their functionalization by deprotometalation/trapping sequences has rarely been explored. In 2000, Enders and coworkers converted ferrocene ketones to enantiopure hydrazones (e.g., using (*S*)-1-amino-2-methoxymethylpyrrolidine, SAMP) in order to achieve their diastereoselective functionalization by deprotolithiation/trapping sequences [42]. A similar approach was later developed by Top and coworkers using chiral imines derived from ferrocene ketones [43].

To our knowledge, the only study concerning the direct functionalization of ferrocene ketones using lithium bases was reported by Enders and coworkers, who subjected enantiopure diferrocenyl ketones to *s*-BuLi in the presence of *N*,*N*,*N*′,*N*′-tetramethylethylenediamine (TMEDA) in toluene at −78 °C for 9 h, prior to interception with various electrophiles [44]. However, the reactivity of the function toward nucleophiles was probably affected by the presence of the two organometallic cores, and the behavior of this particular substrate may not reflect the behavior of aroylferrocenes in general. Thus, when benzoylferrocene was treated with sodium zincate (TMEDA)Na(TMP)Zn(*t*-Bu)$_2$ [TMP = 2,2,6,6-tetramethylpiperido] in hydrocarbon solvents at room temperature, mixtures of products were observed, some resulting from deprotonation (mediated by TMP) of the ferrocene core at the site adjacent to the ketone, others from competitive 1,2- and 1,6-addition reactions [45].

In 2010, we reported a synthesis of 1-benzoyl-2-iodoferrocene in 36% yield using a base generated in tetrahydrofuran (THF) from LiTMP (1.5 equiv) and $CdCl_2$·TMEDA (0.50 equiv) [46]. Here, our goal is to evaluate an approach using the less toxic $ZnCl_2$·TMEDA for the functionalization of ferrocene ketones and to investigate the development of an enantioselective version.

2. Results and discussion

2.1. *Preliminary considerations*

Our aim in this study was twofold: firstly, to identify suitable conditions to functionalize ferrocene ketones by deprotometalation, and secondly, to understand the regioselectivity observed during this reaction. Indeed, most of the ferrocene ketones studied here have two to four sites that can be functionalized in the presence of organometallic bases.

Our approach involved the use of a hindered lithium amide, LiTMP, in THF containing $ZnCl_2$·TMEDA as an in-situ trap [47]. While many deprotometalations using lithium dialkylamides are under thermodynamic control [48], those using the strong base LiTMP can also lead to derivatives functionalized next to a coordinating element, probably via pre-metalation complexes (complex-induced proximity effect) [49,50] or/and rate-limiting transition states (kinetically enhanced metalation) [51,52], or benefiting from favorable hydrogen charges (overriding base mechanism) [53–56]. This is particularly true when using an in-situ trap, as we intended to do.

Therefore, to get an idea of the kinetic acidity of the ferrocene ketones selected for the present study, we calculated (see computational details in Supplemantary material) the atomic charges of a few representative examples by natural population analysis (NPA), with and without oxygen coordination to lithium of $LiNMe_2$ chosen as model base. For benzoylferrocene (**1-Ph**), the most acidic hydrogens were found on the substituted cyclopentadienyl ring of ferrocene, on either side of the benzoyl group (Figure 1, **1-Ph**). Further calculations of NPA charges

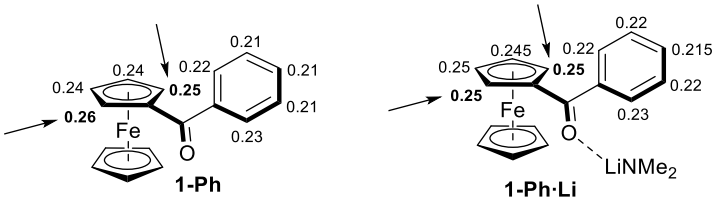

Figure 1. Natural-population-analysis charges on hydrogen atoms in the isolated molecule of benzoylferrocene (**1-Ph**) and impact of coordination to lithium on these charges (complex of **1-Ph** with $LiNMe_2$).

for all hydrogen atoms of the two substituted rings of the complex **1-Ph·Li** showed comparable results (Figure 1, **1-Ph·Li**). A similar tendency was observed for the other substrates (Figure S1, in Supplementary material).

However, formation of the thermodynamic product can also be observed in reactions using strong lithium dialkylamides such as LiTMP [57–59]. We therefore also calculated significant pK_a values for several aroyl ketones in THF within the DFT framework [60–63] (see Figure S2 in Supplementary material for a complete list). As shown on Figure 2a, the lowest pK_a value for **1-Ph** corresponds to the ferrocene site next to the carbonyl group. Coordinating the ketone to $LiNMe_2$ (**1-Ph·Li**, to mimic the stabilizing effect that the function exerts on the lithiated derivative formed) also seemed to show that the most stable lithium species was the one deprotonated next to the carbonyl group on the ferrocene side (Figure 2a, **1-Ph·Li**).

The introduction of electron-withdrawing substituents such as Br or CF_3 on the phenyl group (with compounds **1-*p*BrPh** and **1-*p*CF$_3$Ph**) significantly decreased the pK_a values at their adjacent positions (Figure 2b). However, coordination to $LiNMe_2$ restored the desired reactivity, and the species deprotonated on the ferrocene side appeared to be the most stable. A similar, although less pronounced, effect can be noticed for **1-*p*OMePh** (Figure 2c). Finally, in the case of (2-pyridoyl)- and (2-benzothienoyl)ferrocenes (**1-2Py** and **1-2BTh**), the calculations showed different behaviors, with lithium derivatives being more stable when deprotonation occurs on the heterocycle side (Figure 2d). Furthermore, unlike the other benzoylferrocene compounds considered, the conformation adopted by these heterocyclic compounds has a clear impact on their computed pK_a values (see Figures S3 and S4 in Supplementary material).

All these data suggest that it should be possible to functionalize most of these derivatives next to the ketone on the ferrocene core, while (heteroaroyl)ferrocenes could afford derivatives functionalized on the heterocycle side. With these predictions in mind, we then subjected our selected compounds to the planned deprotometalation/trapping sequences.

2.2. *Functionalization of ferrocene ketones*

Various ferrocene ketones have been prepared in the frame of this study (for details, see Supplementary material). Most of the aroylferrocenes were obtained by Friedel–Crafts acylation, by adapting reported procedures [64–66]. A few other ferrocene ketones were synthesized either by action of lithioferrocene onto the Weinreb 2,2,2-trifluoroacetamide (compound **1-CF$_3$**; see Scheme 7) [67] or by reacting heteroarylmetals with the Weinreb amide of ferrocene [68] (compounds **1-2Py** and **1-2BTh**).

Benzoylferrocene (**1-Ph**) was chosen to optimize the reaction using LiTMP in the presence of an in-situ trap [47]. We first tested the use of the putative $Zn(TMP)_2$ (generated from 1 equiv of $ZnCl_2$·TMEDA and 2 equiv of LiTMP) as an in-situ trap [69] in the reaction of **1-Ph** with LiTMP (1.1 equiv) in THF at −20 °C. After subsequent trapping with iodine, the expected product **2-Ph** was obtained in a moderate 55% yield although almost complete conversion was obtained (<4% **1-Ph** recovered). Replacing $Zn(TMP)_2$ with $ZnCl_2$·TMEDA (1.1 equiv) favored the formation of **2-Ph**, isolated in 72% yield (91% using 2.2 equiv of LiTMP) (Scheme 1, Equation (1)). The intermediate ferrocenylzinc was also engaged in a Negishi cross-coupling [70,71] with 2-chloropyridine. Thus, the use of catalytic amounts of $PdCl_2$ and 1,1′-bis(diphenylphosphino)ferrocene

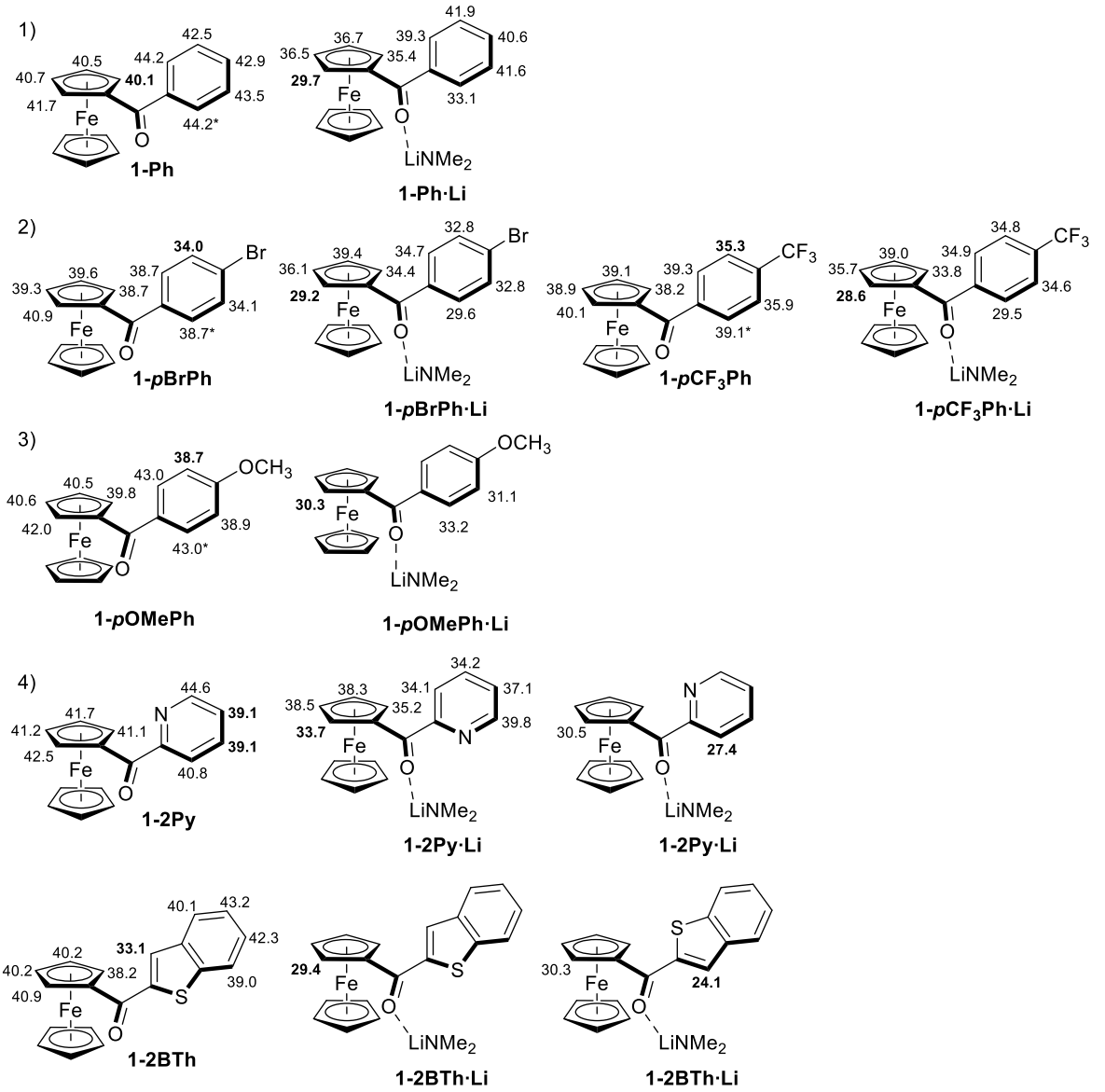

Figure 2. Values of pK_a calculated for ferrocene ketones in THF (an asterisk means that deprotonation in the corresponding position is predicted to lead to interring rotation in order to reduce electron repulsion), and impact of coordination to lithium on these values (complexes with $LiNMe_2$).

(dppf) [72] led to the expected heteroarylated product **3-Ph** (37% yield) (Scheme 1, Equation (2)).

We next attempted to use chlorotrimethylsilane instead of $ZnCl_2$·TMEDA as the in-situ trap, but we failed to observe the formation of the expected ferrocenylsilane under these conditions. We also tried to replace benzoylferrocene (**1-Ph**) by (phenylcarbonothioyl)ferrocene (**4-Ph**), prepared by reacting the former with Lawesson's reagent [73]. However, as already observed in the case of thionoesters [74], the iodinated derivative was not detected, while we recovered 20% of **4-Ph** and 29% of **1-Ph**.

Functionalization at position C-2 of aroylferrocenes was then carried out starting from three different (methoxybenzoyl)ferrocenes, e.g., **1-*o*OMePh**, **1-*m*OMePh**, and **1-*p*OMePh**. As shown in Scheme 2,

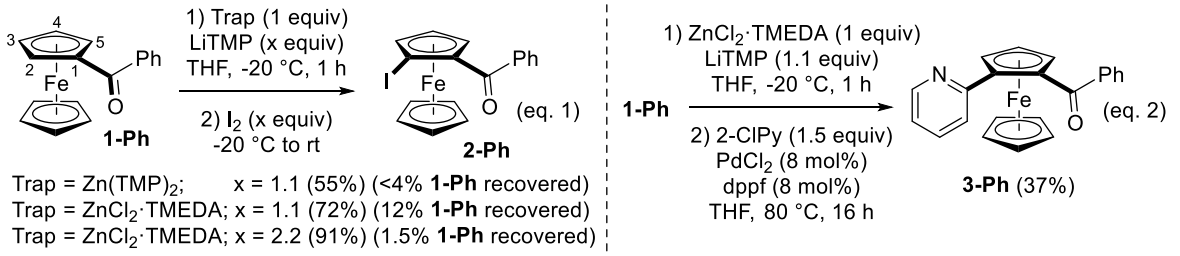

Scheme 1. Functionalization of benzoylferrocene (**1-Ph**) by deprotolithiation with in-situ trap, followed by either iodination or Negishi cross-coupling.

the amount of base was advantageously increased from 1.1 to 1.5 equiv, enabling the isolation of iodides **2-*o*OMePh**, **2-*m*OMePh**, and **2-*p*OMePh** in yields ranging from 82 to 94%. Functionalization of (methoxybenzoyl)ferrocenes at C-2 is therefore consistent with the calculated pK_a values of **1-*p*OMePh** after coordination to lithium (Figure 2c). In the case of (4-*tert*-butylbenzoyl)ferrocene (**1-*pt*BuPh**), derivative **2-*pt*BuPh** was produced in a high 94% yield using 2 equiv of base. Even for the (chlorobenzoyl)ferrocenes **1-*o*ClPh**, **1-*m*ClPh**, and **1-*p*ClPh**, the functionalization took place at the ferrocene site next to the carbonyl group, producing iodides **2-*o*ClPh**, **2-*m*ClPh**, and **2-*p*ClPh** in yields of 51–64%.

The results were different for the other (halo)benzoylferrocenes. In the (bromoaroyl)ferrocene series, all the derivatives obtained resulted from the functionalization next to the ketone function. However, the iodoferrocenes were formed less efficiently (**2-*o*BrPh** > **2-*m*BrPh** > **2-*p*BrPh**), and iodination of the aryl ring was even mainly observed in the case of **2-*p*BrPh** (**2′-*p*BrPh**, >50% yield; Scheme 3). This outcome could be rationalized by the combined effects of the ketone function, which promotes deprotolithiation at its neighboring sites, and bromine, which exerts a long-range acidifying effect [75]. This is consistent with the pK_a values calculated for **1-*p*BrPh·Li**, which are similar for positions C-2 and C-2′ (Figure 2b). A similar trend was noticed in the (trifluoromethyl)ferrocene series, which probably results from the acidifying properties of the trifluoromethyl group in the *ortho*, *meta*, and *para* positions [56,76] (Scheme 3). For **1-*p*CF$_3$Ph·Li**, the pK_a difference between positions C-2 and C-2′ is slightly greater than in the case of **1-*p*BrPh·Li** (Figure 2b), which could explain the predominance of **2-*p*CF$_3$Ph**, functionalized on the ferrocene side.

In contrast to bromine and trifluoromethyl, fluorine is known to be a short-range acidifying group [76,77]. As a consequence, when (2-fluorobenzoyl)ferrocene (**1-*o*FPh**) was treated under the same conditions, the expected product **2-*o*FPh** functionalized on the ferrocene ring (41% yield) was accompanied by (2-fluoro-3-iodobenzoyl)ferrocene (**2′-*o*FPh**, 6% yield) and 1-(2-fluoro-3-iodobenzoyl)-2-iodoferrocene (**2″-*o*FPh**, 18% yield), both due to competitive reactions next to the halogen (Scheme 4).

Coordination of (2-pyridoyl)- and (2-benzothienoyl)ferrocenes (**1-2Py** and **1-2BTh**) to lithium decreases their pK_a values at position C-3′ by several units, making these sites more prone to deprotometalation than those in position C-2 (Figure 2d). For ferrocene **1-2Py**, the calculated pK_a difference is about three units, while it reaches six units for ferrocene **1-2BTh**. As a result, in these two cases, the main products obtained are iodinated on the heterocycle with **2′-2Py** (26% yield) and above all **2′-2BTh** (>50% yield). Products monoiodinated on ferrocene were not observed, but the diiodides **2″-2Py** and **2″-2BTh**, probably resulting from double deprotometalation/trapping, were isolated in ~10% yield (Scheme 5).

Cinnamoyl- and (phenylpropioloyl)ferrocenes (**1-CH=CHPh** and **1-C≡CPh**) were also involved in the reaction for the purpose of comparison with **1-Ph**. The expected products were obtained in both cases, but with lower yields than those observed with **1-Ph**. Compound **2-C≡CPh** was produced in a higher yield (48%) than **2-CH=CHPh** (only 25%), probably due to higher sensitivity of **1-CH=CHPh** (only 17% recovered) to nucleophilic attacks, leading to unidentified decomposition products (Scheme 6).

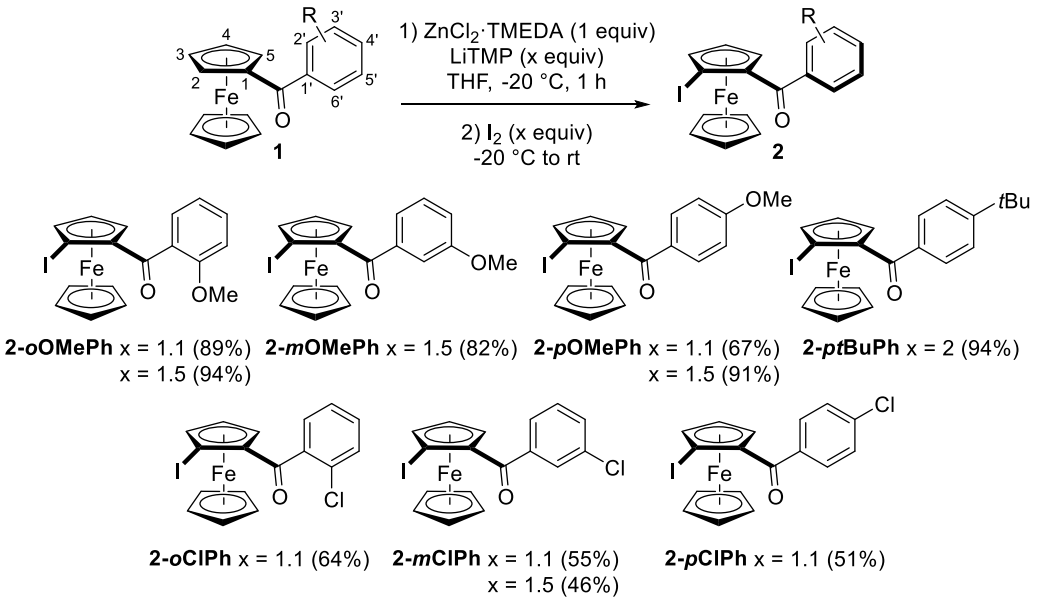

Scheme 2. Regioselective functionalization of aroylferrocenes at C-2 by deprotolithiation with in-situ trap, followed by iodination.

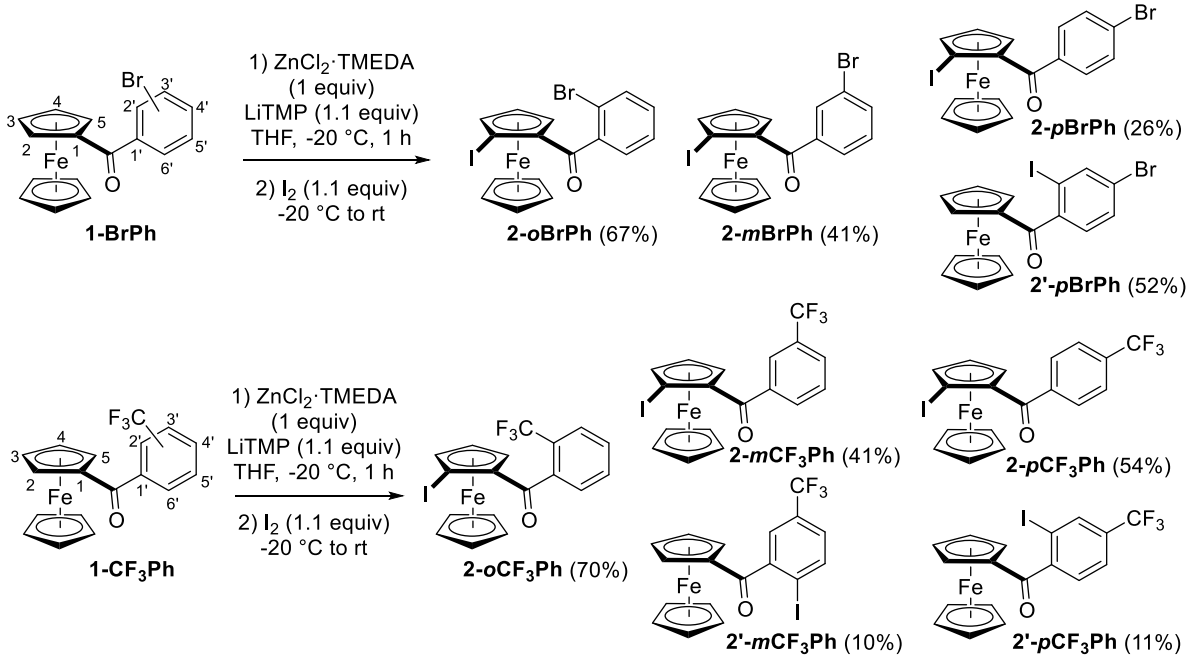

Scheme 3. Functionalization of (bromobenzoyl)- and [(trifluoromethyl)benzoyl]ferrocenes by deprotolithiation with in-situ trap, followed by iodination.

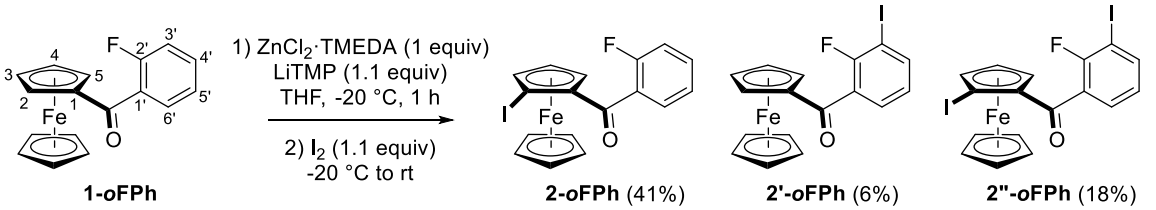

Scheme 4. Functionalization of (2-fluorobenzoyl)ferrocene by deprotolithiation with in-situ trap, followed by iodination.

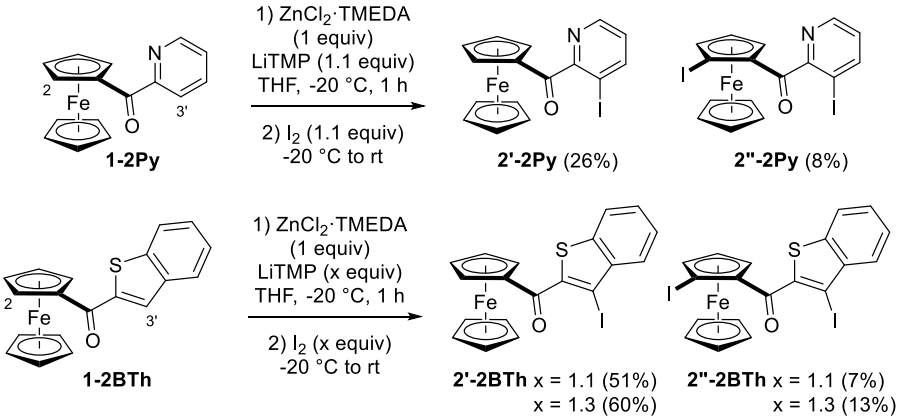

Scheme 5. Functionalization of (2-pyridoyl)- and (2-benzothienoyl)ferrocenes by deprotolithiation with in-situ trap, followed by iodination.

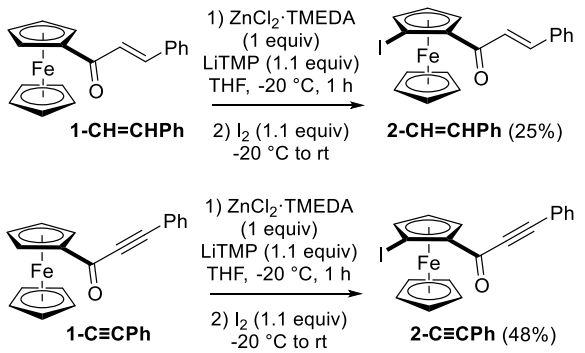

Scheme 6. Functionalization of cinnamoyl- and (phenylpropioloyl)ferrocenes by deprotolithiation with in-situ trap, followed by iodination.

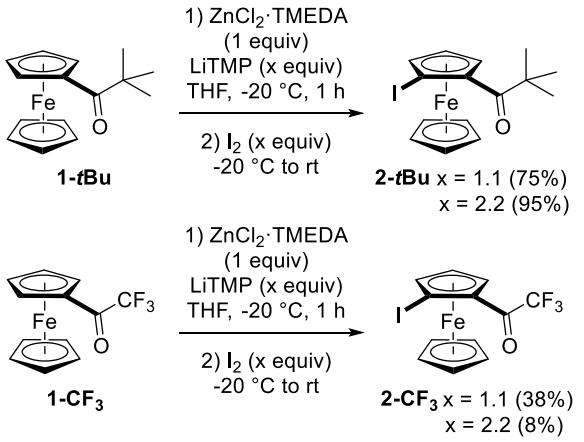

Scheme 7. Functionalization of [(trifluoromethyl)carbonyl]- and (*tert*-butylcarbonyl)ferrocenes by deprotolithiation with in-situ trap, followed by iodination.

Finally, we compared the reactivities of [(trifluoromethyl)carbonyl]ferrocene (**1-CF$_3$**) and (*tert*-butylcarbonyl)ferrocene (**1-*t*Bu**) under these conditions. As the question of regioselectivity does not arise, **1-*t*Bu** was treated with 1.1 or 2.2 equiv of LiTMP to provide, after subsequent trapping, the expected iodide **2-*t*Bu** in high yield (75–95%). However, while the use of 1.1 equiv of LiTMP on **1-CF$_3$** afforded **2-CF$_3$** (as an inseparable mixture with **1-CF$_3$**) in an estimated 38% yield, using an excess of base was detrimental to the reaction outcome (Scheme 7).

Ferrocene ketones being prochiral substrates, their enantioselective functionalization is expected to deliver enantio-enriched 1,2-disubstituted derivatives [78]. Enantioselective deprotolithiation of ferrocenes substituted by aminomethyl [79,80] and dimethylamino [81,82] groups, as well as hindered tertiary carboxamide [83–86] or even triflone [87], using alkyllithium-chiral ligand chelates (e.g., *n*-BuLi-sparteine), represents an important achievement in this field. However, as such chiral nucleophilic bases would be barely compatible with a sensitive ketone, we evaluated another approach involving a chiral, non-nucleophilic lithium dialkylamide {lithium di[(*S*)-1-phenylethyl]amide, (*S*)-PEALi} in the presence of an in-situ trap, as initially documented by Simpkins [88] and later extended to sensitive ferrocene carboxamides and esters [74,89,90]. Regarding the nature of the in-situ trap [91], we selected $ZnCl_2$·TMEDA as well as the putative zinc diamide $\{(S)\text{-PEA}\}_2Zn$, obtained in situ from (*S*)-PEALi and $ZnCl_2$·TMEDA in a 2:1 ratio, given their superiority in studies already carried out in the group [87,92].

To optimize the reaction, a solution of ketone **1-Ph** and $ZnCl_2$·TMEDA (1 equiv) in THF was treated with (*S*)-PEALi (2.2 equiv) at various temperatures (0, −20, −50, and −80 °C) before iodolysis (Scheme 8, Equation (1)). Whereas lower yields of **2-Ph** were recorded at −50 °C and even lower at −80 °C, the best enantioselectivities were observed at 0 or −20 °C but did not exceed 38% enantiomeric excess (*ee*) in favor of the R_P enantiomer, as revealed by the growing of crystals suitable for X-ray diffraction (XRD) analysis (Figure 3). No change in *ee* was noticed by using either (*R*)-PEALi instead of (*S*) or a shorter contact time. We next attempted the reaction using our alternative in-situ trap, $\{(S)\text{-PEA}\}_2Zn$, instead of $ZnCl_2$·TMEDA (Scheme 8, Equation (2)). The reactions were thus repeated at −20 and −80 °C, affording the major R_P enantiomer in a slightly improved 44% *ee* and yields of 60 and 35%, respectively, due to important recovery of **1-Ph** at the lowest temperature. In a last attempt to improve the enantioselectivity, THF was replaced by 2-methyltetrahydrofuran (2-MeTHF), which was found helpful in processes involving sensitive species in asymmetric transformations [93]. However, whether using $ZnCl_2$·TMEDA at −20 °C or $\{(S)\text{-PEA}\}_2Zn$ at −80 °C as an in-situ trap, significantly lower yields (from 69 to 40% and from 35 to 3%, respectively) and enantioselectivities (from 38 to 18% *ee* and from 44 to 4% *ee*, respectively) were recorded.

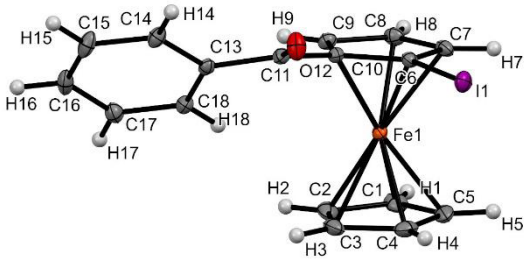

Figure 3. Molecular structure of compound $\boldsymbol{R_P}$**-2Ph** in the solid state. Thermal ellipsoids shown at the 30% probability level. Selected bond lengths (Å) and angles (°): C10–C11 = 1.475(3), C6–I1 = 2.082(2), C10–Cg2···Cg1–C3 = 2.74 (Cg1 being the centroid of the C1–C2–C3–C4–C5 ring and Cg2 the one of the C6–C7–C8–C9–C10 ring), Cg2–C6–I1 = 175.62, C6–C10–C11–O12 = 15.8(4), O12–C11–C13–C14 = 25.9(3).

Reactions using $ZnCl_2$·TMEDA as an in-situ trap, being considerably easier to implement, were performed at −20 °C to explore the behavior of a selection of ferrocene ketones in asymmetric deprotolithiation (Scheme 9). The yields recorded for these reactions using (*S*)-PEALi were generally lower than those obtained with the same amount of LiTMP, which can be explained in most cases by the lower reactivity of (*S*)-PEALi. Using these conditions, ketones **1-CH=CHPh** and **1-C≡CPh** only afforded mixtures of unidentified products. The ferrocenyl versus aryl deprotonation selectivities were the same, notably with the competitive formation of derivatives iodinated on the aryl group in the case of **1-*p*BrPh**, **1-*o*FPh**, **1-*m*CF_3Ph**, and **1-*p*CF_3Ph**. The enantioselectivities remained modest at best, ranging from 0% for the sterically hindered ketone **1-*o*CF_3Ph** to 60% for the trifluoromethylketone **1-CF_3**. Pleasingly, crystallization of **2-*o*BrPh** afforded an enantiopure product (see Supplementary material), and XRD analysis validated the expected R_P configuration.

Slightly disappointed by these results, we next turned our attention to a diastereoselective approach and prepared the enantiopure ferrocene ketone $\boldsymbol{R_P}$**-5** from [(*S*)-1-(dimethylamino)ethyl]ferrocene (Ugi's amine) [94,95] (Scheme 10). Further treatment of $\boldsymbol{R_P}$**-5** with LiTMP (2 equiv) in THF containing $ZnCl_2$·TMEDA (1 equiv) at −20 °C before iodolysis afforded the expected iodoferrocene $\boldsymbol{R_P}$**-6** as a single diastereoisomer, albeit in a low 20% yield due

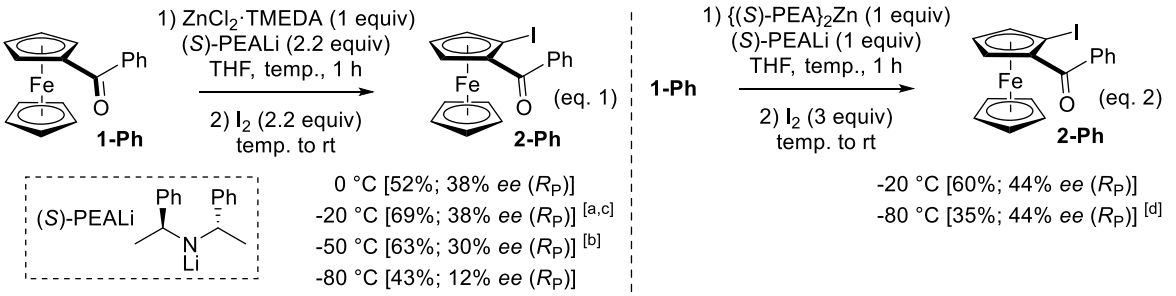

Scheme 8. Enantioselective functionalization of benzoylferrocene (**1-Ph**) by deprotolithiation using the lithium di(1-phenylethyl)amide (*S*)-PEALi with zinc-based in-situ traps. (a) 67% yield and 38% *ee* (S_P) using (*R*)-PEALi. (b) 62% yield and 30% *ee* (R_P) after 5 min time. (c) 40% yield and 18% *ee* (R_P) using 2-MeTHF. (d) 3% yield and 4% *ee* (R_P) using 2-MeTHF.

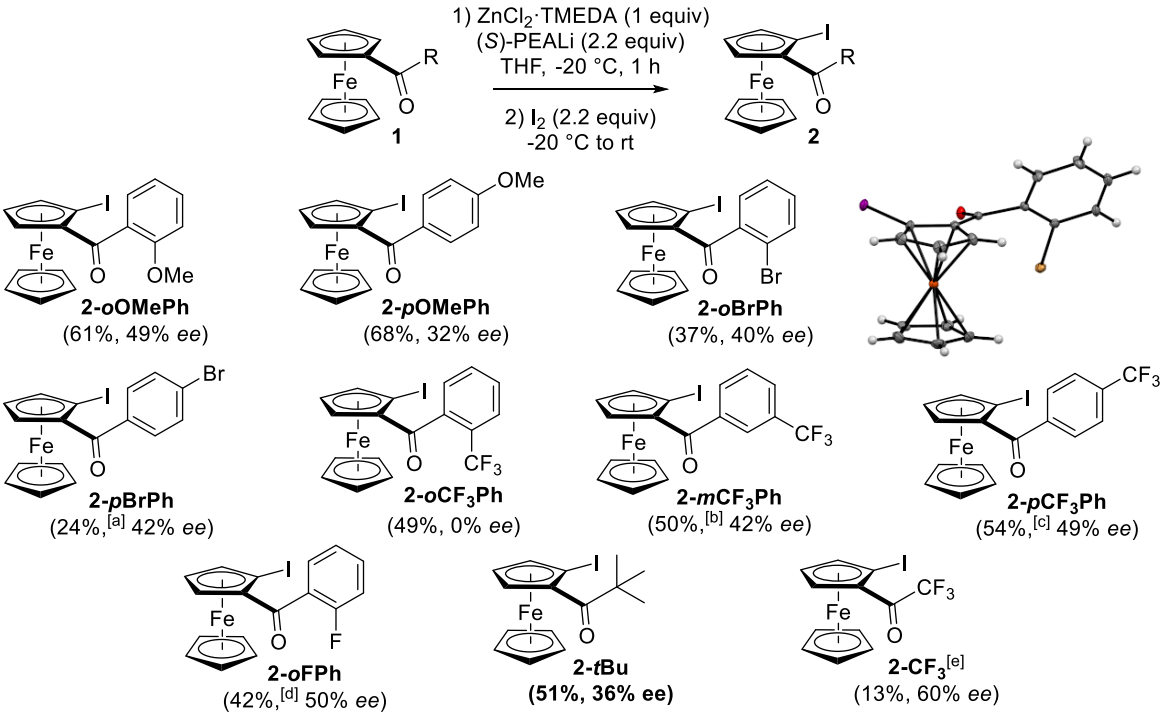

Scheme 9. Enantioselective functionalization of ferrocene ketones by deprotolithiation using the lithium di(1-phenylethyl)amide (*S*)-PEALi with $ZnCl_2$·TMEDA as an in-situ trap. (a) **2′-*p*BrPh** also obtained in 50% yield. (b) **2′-*m*CF$_3$Ph** also formed in 8% yield. (c) **2′-*p*CF$_3$Ph** also formed in 16% yield. (d) **2′-*o*FPh** (23% yield) and **2″-*o*FPh** (15% yield, 28% *ee*) also formed. (e) Reaction carried out by using (*S*)-PEALi (1.1 equiv) and I_2 (1.1 equiv).

to recovery of ***R*$_P$-5** (about 20%) and formation of unidentified byproducts (Scheme 10).

In 1991, Olah and co-workers reported the ring *tert*-butylation of benzophenones by successive action of *t*-BuLi in THF at very low temperature and $SOCl_2$ [96]. Inspired by these results, we similarly treated ***R*$_P$-5** with *t*-BuLi at −80 °C for 15 min before addition of I_2 to either intercept a deprotometalated species or oxidize a 1,6-adduct. Pleasingly, we were able to isolate the 1,6-addition/rearomatization product ***R*$_P$-7** in 61% yield (Scheme 11, Equation (1)). A similar result was recorded from benzoylferrocene (**1-Ph**), with **1-*pt*BuPh** obtained in 80% yield (Scheme 11, Equation (2)).

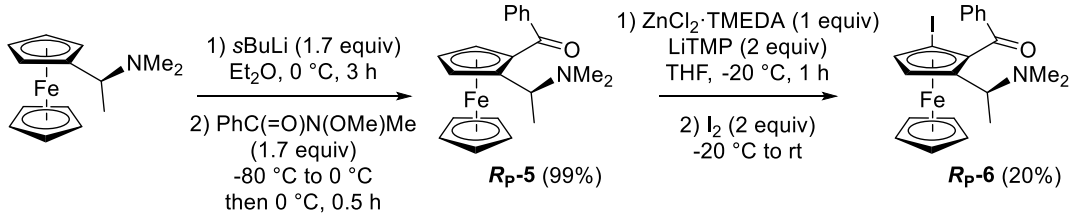

Scheme 10. Diastereoselective conversion of Ugi's amine to the ketone R_P-**5** and further conversion to the enantiopure iodoketone R_P-**6**.

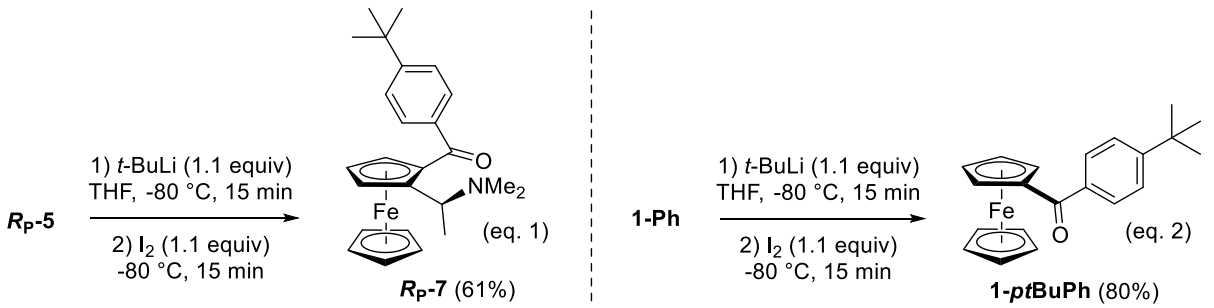

Scheme 11. Ring *tert*-butylation of R_P-**5** and **1-Ph**.

In the course of their studies on the reactivity of organolithium compounds toward ketones, Yamataka and coworkers obtained both the products coming from the 1,2-addition (65%) and the 1,6-addition/rearomatization (28%) by reacting benzophenone with *t*-BuLi in Et_2O at 0 °C [97]. The use of various *tert*-butylzinc species in order to achieve *para*-selective *tert*-butylation of benzophenone [98–100] and other (hetero)aromatic ketones [101] has also been extensively studied. In our case, the major 1,6-addition observed by simply using *t*-BuLi could be explained by the lower electrophilicity of the ketone and the higher steric hindrance generated by the ferrocene core when compared with benzophenone.

Whether using *t*-BuLi [97] or *tert*-butylzinc species [102], all the studies of this reaction have pointed out a single electron transfer mechanism from the alkylmetal to the ketone. Applied to **1-Ph**, the formation of **1-*pt*BuPh** could unfold as depicted in Scheme 12.

2.3. *Post-functionalization toward polycyclic compounds*

Some of our iodinated ferrocene ketones were next engaged in metal-promoted transformations, and post-functionalization by Suzuki–Miyaura cross-coupling [103,104] was first considered from **2-Ph**. The reactions were carried out with 4-methoxyphenyl- and 3-thienylboronic acid, under conditions previously tested [105,106] (2 equiv CsF [107], 5 mol% $Pd(dba)_2$ (dba = dibenzylideneacetone) and 20 mol% SPhos (2-(dicyclohexylphosphino)-2′,6′-dimethoxybiphenyl) [108] in refluxing toluene), to afford the derivatives **8a** and **8b** (Scheme 13, Equation (1) and (2)). A Sonogashira cross-coupling [109] was next attempted with (trimethylsilyl)acetylene, under conditions previously reported [40,110] [4 mol% $Pd(PtBu_3)_2$ and 4 mol% CuI in THF-iPr_2NH at rt]. Although the expected product **9** was obtained in a low 21% yield due to 55% recovery of **2-Ph** (Scheme 13, Equation (3)), it could be a promising substrate for accessing biologically active ferrocene derivatives such as prostaglandin analogues [111].

In the last decade, ferrocenes fused with heterocycles such as pyridine [112], 4-pyridone [112], and 4-piperidinone [113] have appeared as privileged structures for different applications [114]. With the aim of preparing a sulfur-containing related compound and inspired by similar reaction in the benzene series [115], we reacted

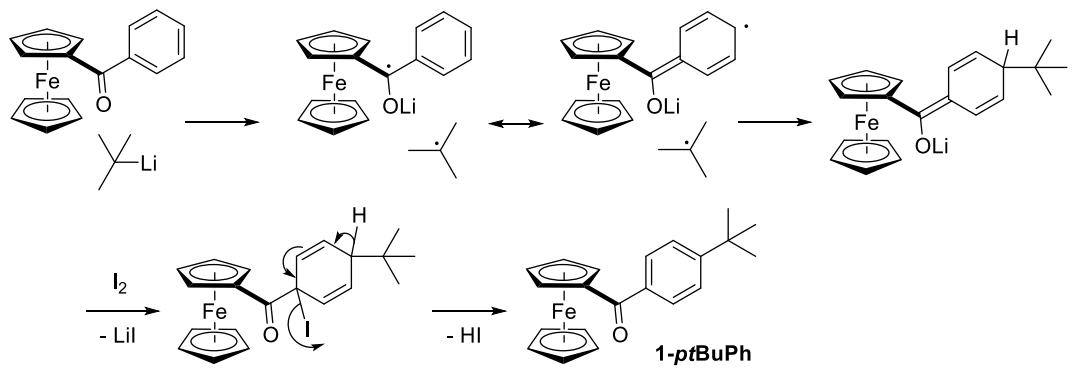

Scheme 12. Proposed mechanism for the *tert*-butylation of **1-Ph**.

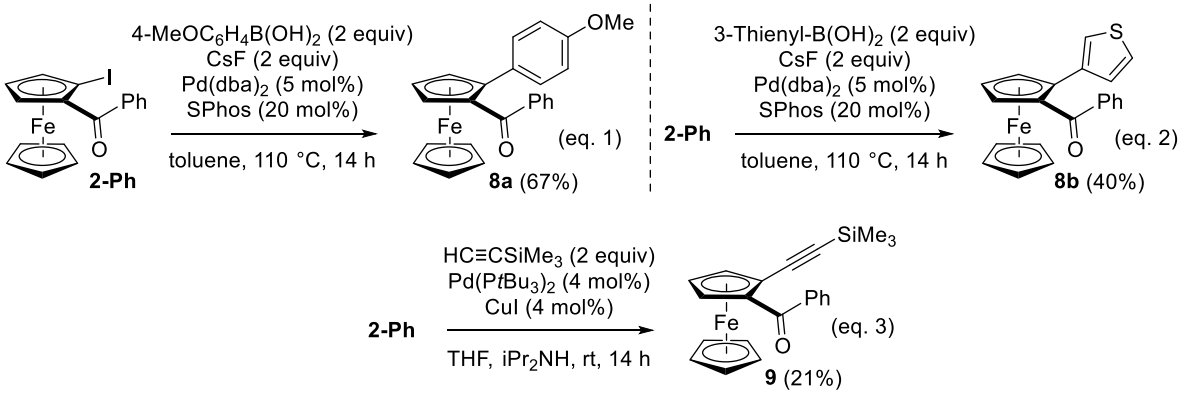

Scheme 13. Suzuki–Miyaura and Sonogashira cross-coupling reactions from **2-Ph**.

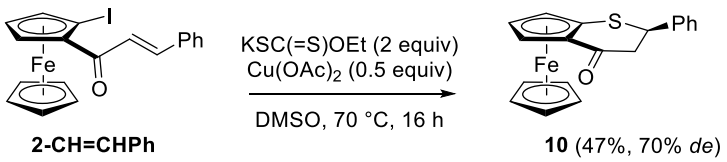

Scheme 14. Conversion of **2-CH=CHPh** to the 2,3-dihydrothiopyrano[2,3]ferrocen-4-one **10**.

(*E*)-1-cinnamoyl-2-iodoferrocene (**2-CH=CHPh**) with potassium ethyl thioxanthate in the presence of $Cu(OAc)_2$ in dimethylsulfoxide (DMSO) at 70 °C. Pleasingly, we were able to isolate the expected 2,3-dihydrothiopyrano[2,3]ferrocen-4-one **10** in 47% yield and 70% *de* (Scheme 14).

Ferrocene-fused quinoline derivatives are also documented, and notably ferroceno[*c*]quinolines, which can be synthesized from 2-iodoferrocene carboxaldehyde [116]. As starting from a ketone would provide a substituent in position C-6 of this building block, we were keen to prepare such derivatives from the iodinated ketone **2-*p*CF_3Ph**. Inspired by previous results, it was treated with 4 equiv of 2-aminophenylboronic acid, 5 mol% $Pd(dba)_2$, 20 mol% PPh_3, and 2 equiv of CsF [107], to which 2 equiv of Cs_2CO_3 were added for subsequent cyclization in refluxing dioxane. This afforded the original compound **11** in high yield (Scheme 15).

Condensed systems in which the cyclopentadienyl ring of the ferrocene is annulated with a (hetero)aromatic moiety have seen renewed interest with

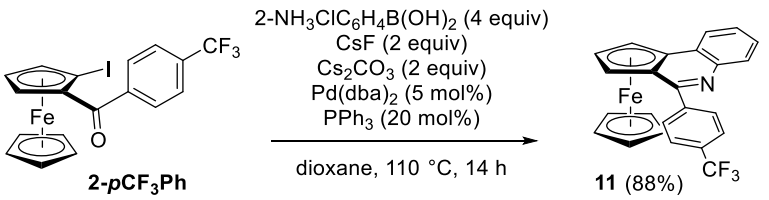

Scheme 15. Suzuki–Miyaura cross-coupling from **2-*p*CF$_3$Ph** and subsequent cyclization into ferroceno[*c*]quinoline.

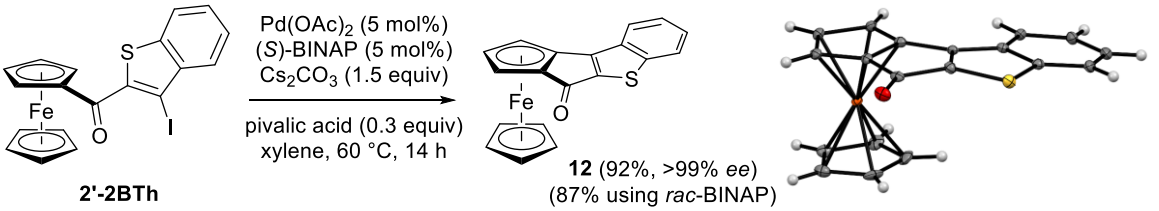

Scheme 16. Conversion of **2′-2BTh** to the polycyclic compound **12** by CH-functionalization.

the advent of palladium-catalyzed enantioselective C–H bond activation [114]. Inspired by the synthesis of ferrocene analogues of fluorenone documented by You and coworkers [117], we finally attempted the synthesis of the original thiophene-containing derivative **12** from the iodinated compound **2′-2BTh**. To this purpose, our substrate was treated with 5 mol% $Pd(OAc)_2$, 5 mol% (*S*)-BINAP [BINAP = 2,2′-bis(diphenylphosphino)-1,1′-binaphthyl], 1.5 equiv of Cs_2CO_3, and 0.3 equiv of pivalic acid in xylene at 60 °C. Pleasingly, the expected tetracyclic compound **13** was isolated in 92% yield and >99% *ee*, the R_P absolute configuration being confirmed by XRD analysis (Scheme 16).

2.4. *Electrochemical characterization of selected compounds*

Although ferrocene ketones have been known since the early days of ferrocene history [41], and indeed helped Woodward and his team to coined the name ferrocene [118,119], they have been scarcely studied from an electrochemical point of view. Kutal et al. reported an in-depth study of the link between the spectroscopic properties and their electronic structure [120], while Gao et al. reported third-order non-linear optical properties of some benzoylferrocenes, supported by DFT calculations [121]. However, electrochemical analyses were not included in these studies. The redox potential of a few ferrocene ketones has been reported from time to time [122–124], most of the work on benzoylferrocenes coming from the work of Kleinberg et al. [125]. We were therefore interested in investigating the electrochemical properties of some ferrocene ketones prepared during this work, initially focusing our attention on the ketone reduction. Cyclic voltammetry (CV) and differential pulse voltammetry (DPV) were therefore realized in dry, oxygen-free, dimethylformamide, using *n*-Bu_4NPF_6 (0.1 M) as the supporting electrolyte with a glassy carbon disk as working electrode, an Ag/AgCl reference electrode, and a glassy carbon rod as counter electrode (Table 1).

From benzophenone to **1-Ph**, **1-*p*OMePh**, and **1-*t*Bu**, the monoelectronic reduction of the ketone, forming the radical anion species, was found reversible and increasingly difficult to achieve, in agreement with the increased electron-donating properties of the group attached to the ketone. Regarding the effect of electron-withdrawing groups, reduction is easier from the 2-pyridyl derivative **1-2Py** than from the compounds **1-*p*CF$_3$Ph** and **1-Ph**, as one can have expected regarding the electronic properties of these aromatics. We also attempted to push the reduction of **1-*p*CF$_3$Ph** forward to form the corresponding dianion species. However, although we did observe a second reduction in DPV (see Supplementary material), it did not appear to be the expected formation of the dianion species, but rather the reduction of the trifluoromethyl group,

Table 1. Electrochemical data (in V) for the monoelectronic reduction of selected ferrocene ketones

Compound	E_{pc}[a]	E_{pa}[a]	i_{pc}/i_{pa}[a]	$E_{1/2}$[b]
Benzophenone	−1.74	−1.64	1.00	−1.68
1-Ph	−1.88	−1.79	0.99	−1.84
1-*p*OMePh	−2.00	−1.87	1.36	−1.95
1-*p*CF$_3$Ph	−1.67	−1.51	nd[(c)]	−1.75
1-2Py	−1.68	−1.60	1.43	−1.64
1-*t*Bu	−2.29	−2.15	1.20	−2.23
2-Ph	−1.70	nd[(d)]	nd[(d)]	−1.68
12	−1.36	−1.26	0.92	−1.30

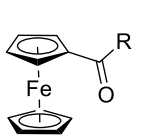

1-Ph R = Ph
1-*p*OMePh R = C_6H_4-4-OMe
1-*p*CF$_3$Ph R = C_6H_4-4-CF_3
1-2Py R = 2-Py
1-*t*Bu R = *t*Bu

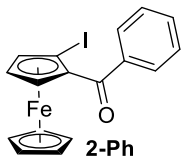

2-Ph

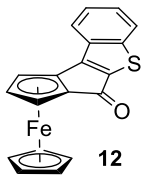

12

Potential values given relative to Ag/AgCl, scan rate = 100 mV·s^{-1}. [a]From CV experiments. [b]From DPV experiments. [c]A complex reduction process was observed. [d]An irreversible dielectronic reduction process was observed.

as reported by Perichon et al. and Savéant et al. [126,127]. Due to the inductive effect of iodine, **2-Ph** was more easily reduced than benzoylferrocene (**1-Ph**) by 0.16 V. However, the first dielectronic irreversible process was immediately followed by a second reduction at −1.84 V versus FcH/FcH$^+$, corresponding to that of **1-Ph**. We suggest that the initial formation of the radical anion of **2-Ph** was followed by the cleavage of the carbon–iodine bond toward the neutral radical **1-Ph$^\bullet$**, which was more easily reduced than the parent compound **2-Ph** (Scheme 17). The resulting anion **1-Ph**$^-$ would then be protonated in situ to generate **1-Ph**, which exhibited the expected monoelectronic reduction at −1.84 V. The fused tetracycle **12** was found to undergo an easy and reversible monoelectronic reduction first, followed by two irreversible reduction peaks, which might be attributed to the reduction of the radical anion to the corresponding dianion and to the reduction of the benzothiophene core [128].

We next investigated the oxidation of the organometallic core for the same compounds but working in dichloromethane this time, in line with our previous studies [92,129] (Table 2). The redox potential of **1-Ph** was measured first, and the 0.25 V value versus FcH/FcH$^+$ was found in good agreement with the results of Herberhold and Jahn, although their measurements were done in acetonitrile instead of dichloromethane [123,124]. As expected, the redox potential of **1-Ph** falls between the ones of **1-*p*OMePh** and **1-*p*CF$_3$Ph** due to their respective electron-donating and electron-withdrawing groups attached to the phenyl ring. The thioketone **4-Ph** was more easily oxidized than the parent ketone ($E_{1/2}$ 0.22 versus 0.25 V), probably due to the stronger electron-withdrawing properties of the former [130]. Surprisingly, the redox potential of the pyridyl derivative (**1-2Py**) was 50 mV lower than that of benzoylferrocene (**1-Ph**). Indeed, due to the more pronounced electron-withdrawing properties of the pyridine ring, the reverse order was expected. However, electronic repulsion between the lone pairs of the ketone and the pyridine's nitrogen might promote a conformation similar to the one observed for **2-2Py** (see below), avoiding the full transmission of the pyridine's electronic effect to the ferrocene core. The ferroceno[*c*]quinolines **11** was found easier to oxidize than any of the ferrocene ketones studied, probably due to the planar structure of the tricyclic core and to the presence of an imine instead of a ketone. In the ferrocene series, it is usually possible to link the $E_{1/2}$ value of monosubstituted derivatives with the Hammett's parameter α_p [122,131,132] and the $E_{1/2}$ of polysub-

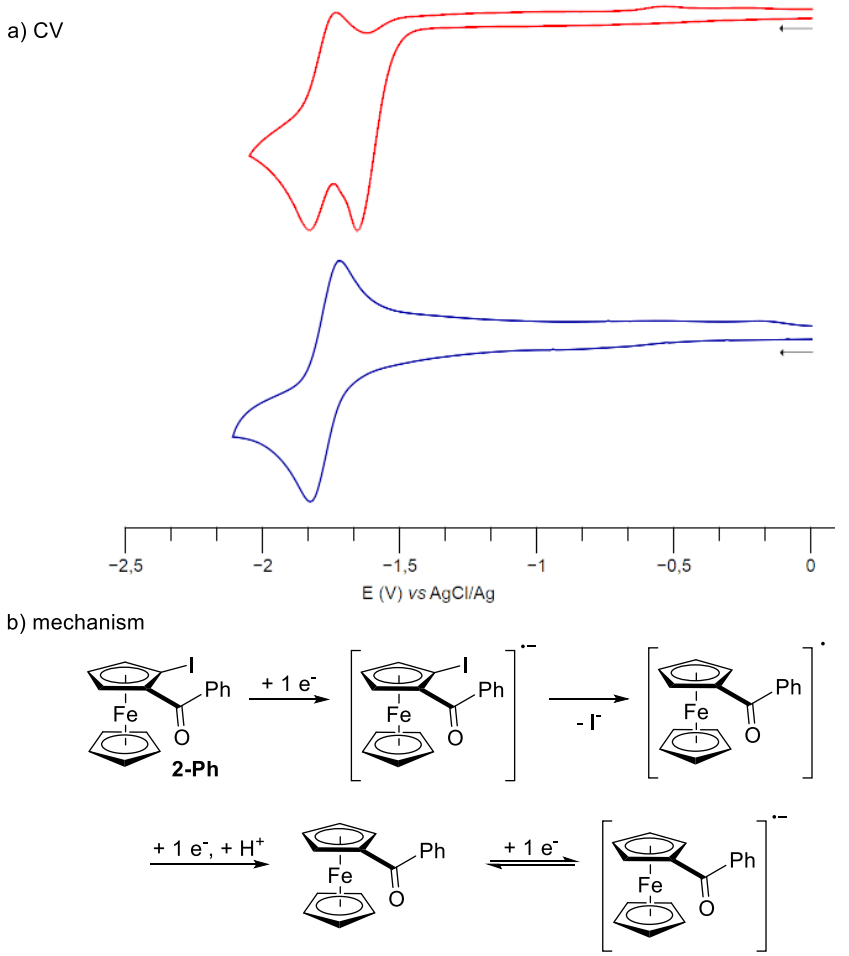

Scheme 17. (a) Cyclic voltammetry of compounds **2-Ph** (red) and **1-Ph** (blue). (b) Putative mechanism for the electrochemical conversion of **2-Ph** into **1-Ph**.

stituted compounds with the sum of α_p or $\alpha_p + \alpha_m$, depending on the substation pattern [133–135]. Unfortunately, only a limited number of Hammett's parameters is known for ketones [130]. However, it was still possible to find a correlation between the recorded $E_{1/2}$ values and the sum of α_p parameters for compounds **1-*t*Bu**, **1-Ph**, **2-Ph**, and **1-CF$_3$** with the equation $E_{1/2} = 1.8466\ \Sigma\alpha_p - 0.026$ ($R^2 = 0.9857$) (see Supplemtary material).

2.5. *Solid-state structures and weak interactions of some ferrocenyl ketones*

In the frame of this work, many ferrocene ketone derivatives were found to produce crystals suitable for XRD analysis, some of them deserving additional comments. Regarding unsubstituted ferrocene ketones, an eclipsed conformation of the ferrocene core was identified in most cases and the substitution pattern of the phenyl ring was found to have an impact on the solid-state structure. For *para*- and *meta*-substituted aromatics, the C=O bond was found tilted above the substituted cyclopentadienyl (Cp) ring while the phenyl ring was slightly inclined compared to the C=O bond. However, for *ortho*-substituted aromatics, the carbonyl was found aligned with the Cp ring while the aromatic was much more tilted, probably to reduce the steric clash between the carbonyl group and the *ortho* substituent. The case of the three trifluoromethylated derivatives is especially representative of this general trend (Figure 4).

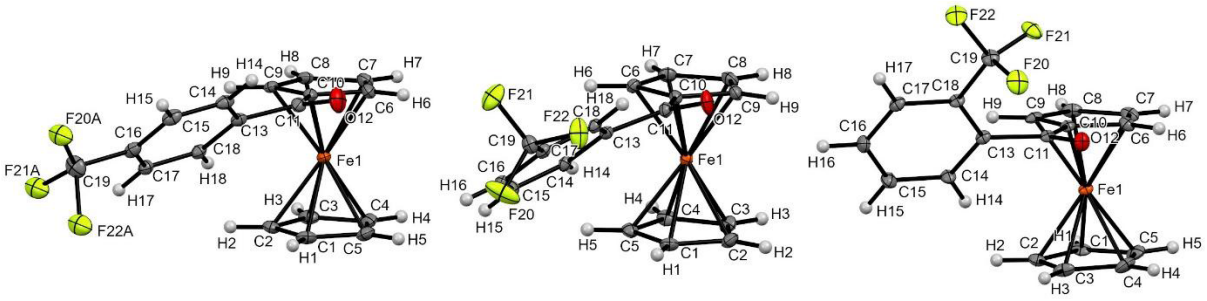

Figure 4. Molecular structure of compounds **1-*p*CF$_3$Ph** (left), **1-*m*CF$_3$Ph** (middle), and **1-*o*CF$_3$Ph** (right) in the solid state. Thermal ellipsoids shown at the 30% probability level. Selected bond lengths (Å) and angles (°) for **1-*p*CF$_3$Ph**: C10–C11 = 1.469(4), C10–Cg2···Cg1–C1 = 4.71 (Cg1 being the centroid of the C1–C2–C3–C4–C5 ring and Cg2 the one of the C6–C7–C8–C9–C10 ring), C6–C10–C11–O12 = 12.9(4), O12–C11–C13–C14 = 27.7(4); for **1-*m*CF$_3$Ph**: C10–C11 = 1.469(3), C10–Cg2···Cg1–C1 = 3.19, C9–C10–C11–O12 = 18.0(3), O12–C11–C13–C18 = 20.2(3); for **1-*o*CF$_3$Ph**: C10–C11 = 1.471(8), C10–Cg2···Cg1–C3 = 7.58, C6–C10–C11–O12 = 2.5(8), O12–C11–C13–C18 = 53.0(7).

Table 2. Electrochemical data (in V) for the oxidation of selected ferrocene ketones

Compound	E_{pa} [a]	E_{pc} [a]	i_{pa}/i_{pc} [a]	$E_{1/2}$ [b]
1-Ph	0.30	0.20	0.88	0.25
1-*p*OMePh	0.27	0.17	0.84	0.21
1-*p*CF$_3$Ph	0.34	0.24	0.75	0.29
1-2Py	0.26	0.17	0.89	0.20
1-*t*Bu	0.25	0.16	0.90	0.22
1-CF$_3$	0.50	0.40	0.81	0.44
4-Ph	0.29	nd[(c)]	nd[(c)]	0.22
2-Ph	0.38	0.29	0.84	0.33
10	0.30	0.20	0.89	0.25
11	0.24	0.14	0.97	0.17
12	0.37	0.28	0.86	0.33

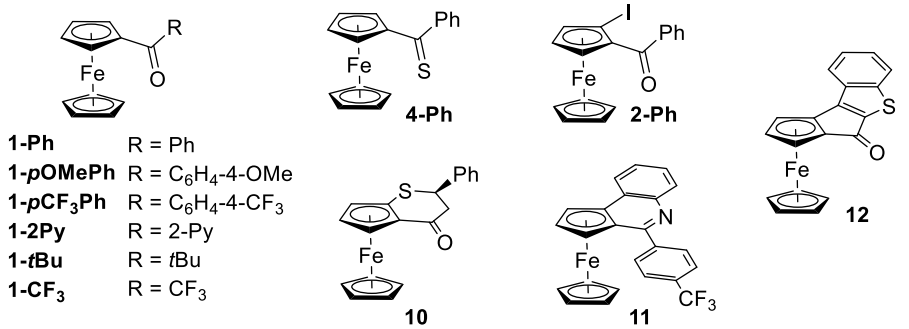

Potential values given relative to FcH/FcH$^+$, scan rate = 100 mV·s^{-1}. [a]From CV experiments. [b]From DPV experiments. [c]Irreversible oxidation was observed.

The iodinated derivative **2′-2Py** further features an intermolecular halogen–oxygen bond resulting from the interaction between the region of positive electrostatic potential (σ-hole) of iodine, acting as the donor, and a lone pair of the oxygen of the ketone, acting as the acceptor [136]. While such interactions

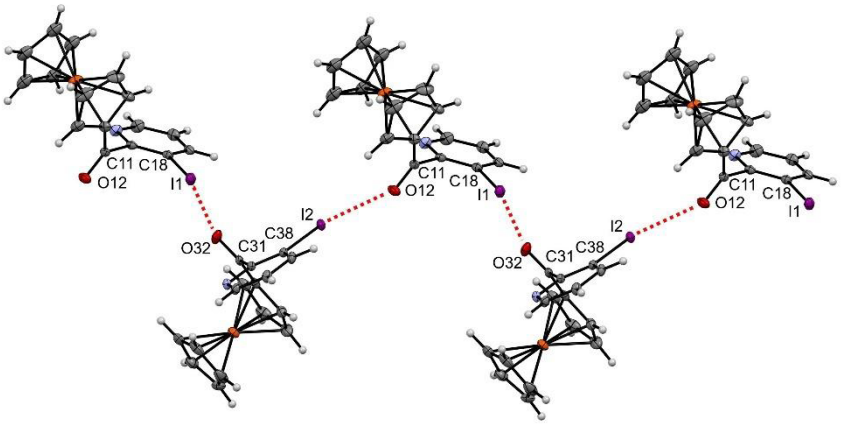

Figure 5. Halogen–oxygen bond observed in the solid state for compound **2′-2Py**. Thermal ellipsoids shown at the 30% probability level. Selected bond lengths (Å) and angles (°) O12···I2 = 3.051, O32···I1 = 3.061, C11–O12···I2 147.99, C31–O32···I1 146.03, O12···I2–C38 156.03, O32···I1–C18 160.76.

are not usually observed with bare iodopyridines, they are more common from iodopyridinium derivatives in which the electron-withdrawing pyridinium ring increases the electrostatic potential of the iodine and thus the strength of the interaction [137,138]. In **2′-2Py**, the ketone adjacent to the iodine atom is expected to have a similar effect, leading to a zigzag halogen-bond network connecting all the molecules in the solid state (Figure 5).

As expected, the introduction of the iodine next to the ketone induced some structural changes in the solid state, as observed between **1-*p*CF$_3$Ph** and **2-*p*CF$_3$Ph** (Figure 6). Indeed, to accommodate the iodine atom, which was inclined by 4.9° above the Cp ring, the C=O bond was forced to move from its tilted position to be aligned with the Cp ring. A large change in the orientation of the phenyl ring was also observed between the two structures.

The substitution pattern of the phenyl ring was also found to influence the solid-state structures of the iodoferrocene ketones. Indeed, except for derivative **2-*p*CF$_3$Ph**, the C=O bond was found tilted from the Cp ring but aligned with the phenyl ring for all the *para*-substituted derivatives, while the contrary was identified for all the *ortho*-substituted derivatives, probably for steric encumbrance reasons. The **2-*p*OMePh** and **2-*o*OMePh** structures depicted in Figure 7 nicely illustrate this trend. The opposite behavior of **2-*p*CF$_3$Ph** might be rationalized in terms of substituent effects. Indeed, due to its strong electron-withdrawing inductive effect, the

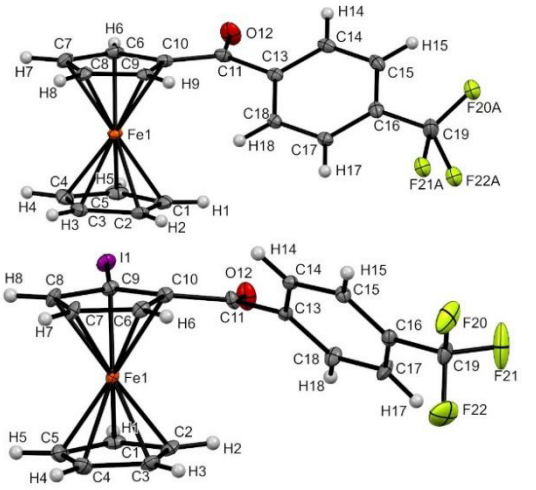

Figure 6. Molecular structure of compounds **1-*p*CF$_3$Ph** (top) and **2-*p*CF$_3$Ph** (bottom) in the solid state. Thermal ellipsoids shown at the 30% probability level. Selected bond lengths (Å) and angles (°) for **2-*p*CF$_3$Ph**: C10–C11 = 1.49(1), C9–I1 = 2.082(7), C10–Cg2···Cg1–C2 = 3.35 (Cg1 being the centroid of the C1–C2–C3–C4–C5 ring and Cg2 the one of the C6–C7–C8–C9–C10 ring), Cg2–C9–I1 = 175.11, C9–C10–C11–O12 = −3(1), O12–C11–C13–C14 = −138.0(8).

trifluoromethyl group might favor the resonance between the Cp ring of the organometallic and the C=O bond, which therefore need to be aligned. For the other *para*-substituted aryl derivatives studied, all substituents have a positive mesomeric effect which might override the donating effect of the ferrocene

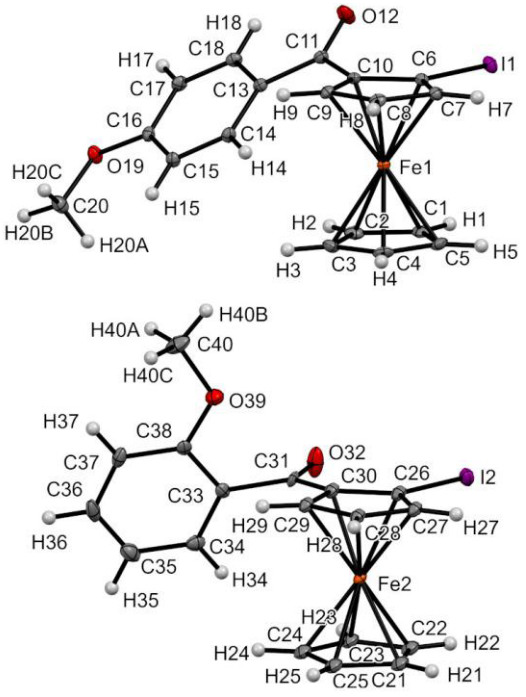

Figure 7. Molecular structure of compounds **2-*p*OMePh** (top) and **2-*o*OMePh** (bottom) in the solid state. Thermal ellipsoids shown at the 30% probability level. Selected bond lengths (Å) and angles (°) for **2-*p*OMePh**: C10–C11 = 1.490(3), C6–I1 = 2.089(2), C10–Cg2···Cg1–C2 = 3.12 (Cg1 being the centroid of the C1–C2–C3–C4–C5 ring and Cg2 the one of the C6–C7–C8–C9–C10 ring), Cg2–C6–I1 = 178.23, C6–C10–C11–O12 = −33.5(3), O12–C11–C13–C18 = −1.1(3); for **2-*p*OMePh**: C30–C31 = 1.492(7), C26–I2 = 2.096(4), C30–Cg4···Cg3–C23 = 22.47 (Cg3 being the centroid of the C21–C22–C23–C24–C25 ring and Cg4 the one of the C26–C27–C28–C29–C30 ring), Cg4–C26–I2 = 176.92, C26–C30–C31–O32 = −10.1(8), O32–C31–C33–C38 = −105.7(7).

core, explaining why the C=O bond is therefore aligned with the phenyl ring.

From racemic **2-*o*ClPh**, preferential crystallization of the enantiopure S_P enantiomer was pleasingly observed [139], allowing us to identify the formation of a halogen–oxygen bond in the solid state (Figure 8). Due to the electron-richness of the organometallic core, iodoferrocenes are usually not able to develop such interactions. However, the presence of electron-withdrawing substituents can substantially increase the positive electrostatic potential of iodine's σ-hole. As a result, halogen bond networks have been recently identified for various iodoferrocenes substituted with sulfonamides [140], sulfonates [92], sulfoxides [141], sulfonyl fluoride [134], and triflones [87]. Similar bonds were also observed for ferrocene iodoalkyne derivatives [142]. In the case of **S_p-2-*o*ClPh**, having the iodine and the ketone groups in a same plane and pointing in the same direction led to a zigzag chain of halogen–oxygen bonds with bonds lengths and angles being in the range of classical values [136].

We were pleased to identify the two types of halogen–halogen interactions in three of our iodoferrocene ketones [143,144]. In the solid state, both enantiomers of **2-*p*ClPh** were identified in the crystal structure, with the R_P enantiomer interacting with the S_P enantiomer via a type II iodine–iodine interaction, characterized by two different C–I···I angle values (Figure 9a). However, while the two enantiomers of **2″-2BTh** crystallized together in a similar manner, a type I iodine–iodine interaction with similar C–I···I angles was observed between the iodine atoms attached to the benzothiophene moiety and not between those linked to the ferrocene core (Figure 9b).

From racemic **2-*o*BrPh**, spontaneous resolution was observed and the two enantiomers were separately isolated as conglomerates. As expected, single molecules of each enantiomer were almost similar in the solid state, both crystallizing in the same tetragonal system, although in different space groups. However, the most interesting characteristics were observed having a closer look at intermolecular halogen–halogen bonds for each enantiomer. Indeed, the bromine of one molecule was found to develop a type I interaction with the iodine atom of another molecule, leading to the helix arrangement of all molecules. While ferrocene derivatives have previously been involved in the formation of such structures [145–148], the involvement of halogen–halogen interactions to structure the arrangement is pretty unusual. The planar chirality of the ferrocene core was further found to influence the axial chirality of the helix, the R_P enantiomer giving rise to a *M* helix (Figure 10a), while a *P* helix was observed for the S_P enantiomer (Figure 10b).

It was finally possible to grow crystals of the enantiopure tetracycle **12** suitable for XRD analysis (Figure 11). Not only the solid-state structure validated the expected R_P configuration of the compound but it also allowed the identification of chalcogen–chalcogen interactions [149,150]. Indeed, a sulfur···sulfur interaction between two

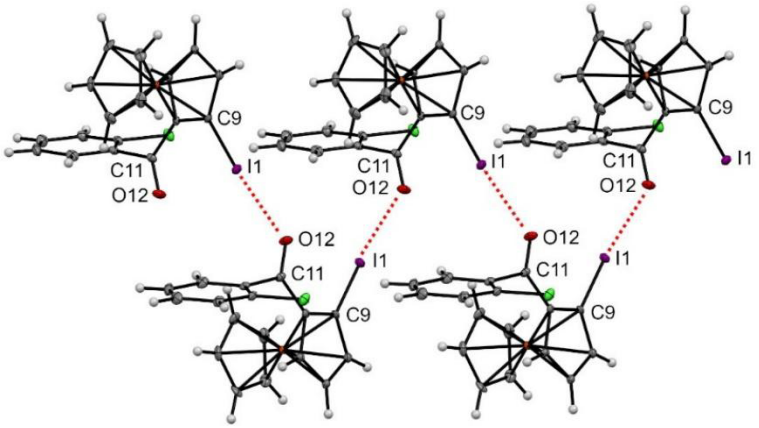

Figure 8. Halogen–oxygen bonds observed in the solid state for compound ***S*p-2-*o*ClPh**. Thermal ellipsoids shown at the 30% probability level. Selected bond lengths (Å) and angles (°) O12···I1 = 2.999, C11–O12···I1 139.63, O12···I1–C9 173.64.

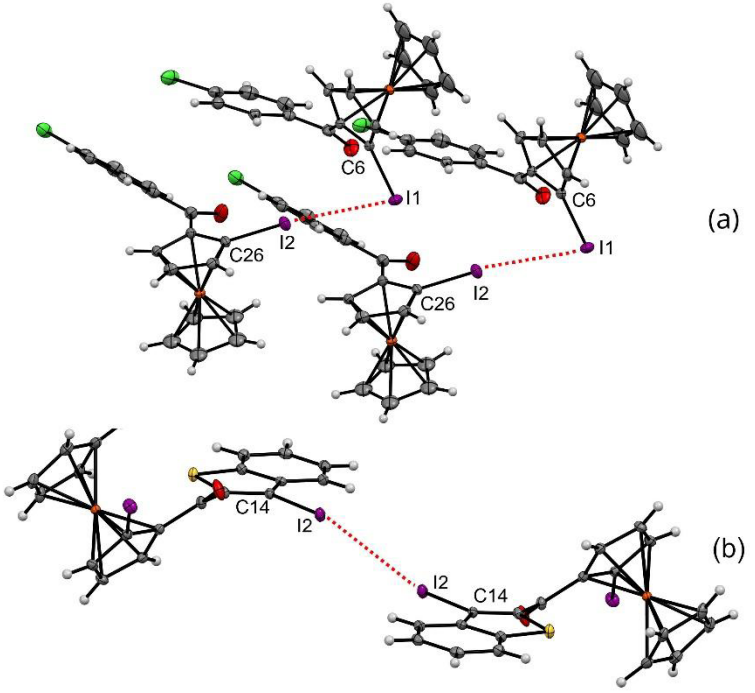

Figure 9. Iodine–iodine interaction network observed in the solid state for compounds **2-*p*ClPh** (top) and **2″-2BTh** (bottom). Thermal ellipsoids shown at the 30% probability level. Selected bond lengths (Å) and angles (°) for **2-*p*ClPh**: I1···I2 = 3.882, I1···I2–C26 173.07, C6–I1···I2 73.43; for **2-*p*ClPh**: I2···I2 = 3.772, I2···I2–C14 137.38, C14–I2···I2 137.38.

molecules was likely to happen due to the S1···S2 distance below the van der Waals radii (3.54 versus 3.60 Å) [151], although the various C–S···S angles are shorter than expected, probably due to the rigid fused-thiophene unit. The tetracyclic systems of the two molecules composing the dimer were found perpendicular and, although this arrangement is not usual, it was previously identified in other benzothiophene derivatives [152].

3. Conclusion

Here we have presented the first in-depth study of the deprotolithiation of ferrocene ketones using a

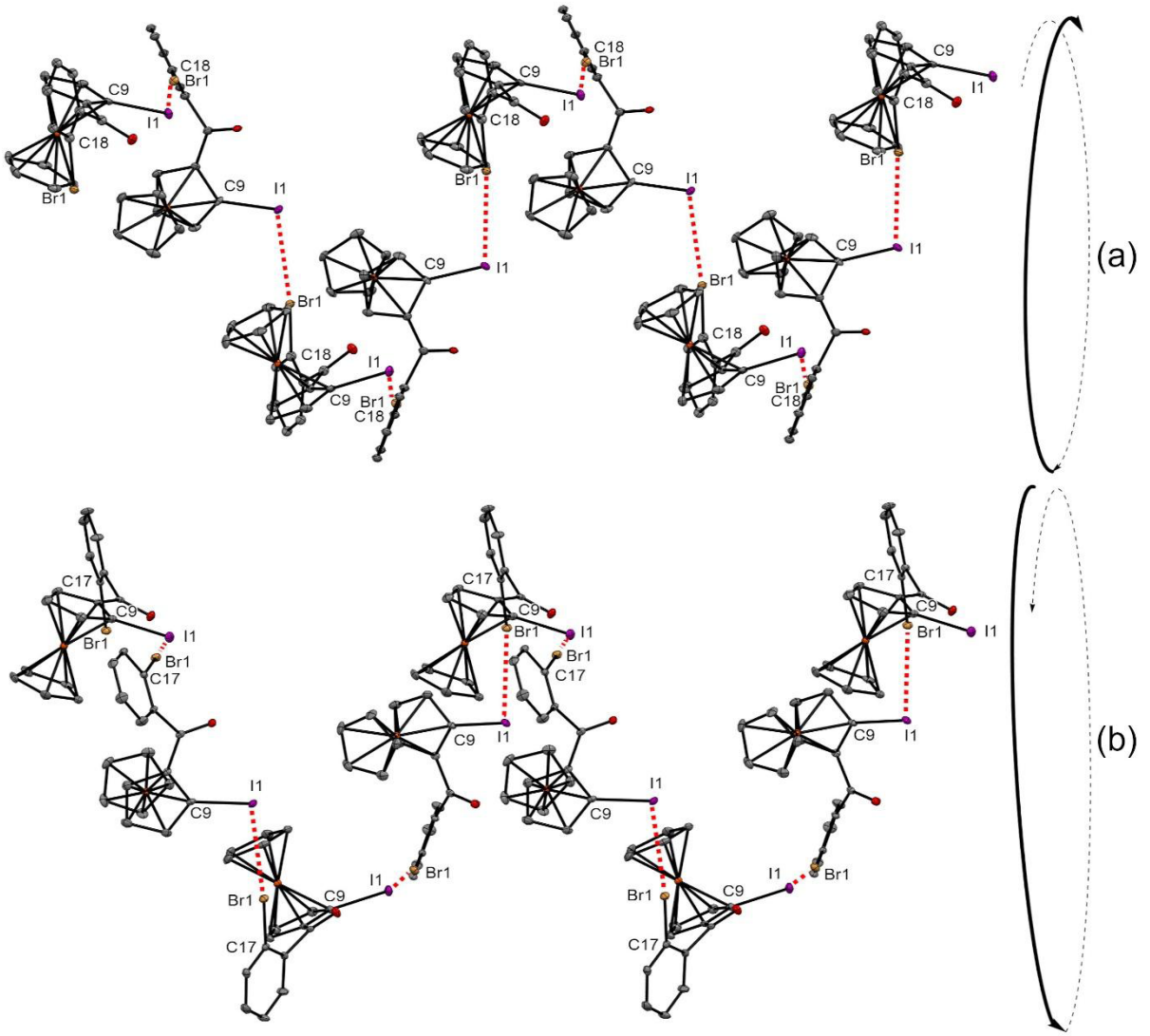

Figure 10. Iodine–bromine bond network observed in the solid state for compounds ***R*p-2-*o*BrPh** (a) and ***S*p-2-*o*BrPh** (b) and sense of the helix formed. Thermal ellipsoids shown at the 30% probability level; hydrogen atoms omitted for clarity. Selected bond lengths (Å) and angles (°) for ***R*p-2-*o*BrPh**: Br1···I1 = 3.594, C18–Br1···I1 171.16, C9–I1···Br1 98.79; for ***S*p-2-*o*BrPh**: Br1···I1 = 3.599, C17–Br1···I1 170.96, C9–I1···Br1 99.35.

bulky, non-nucleophilic lithium amide, as well as an in-situ trap to prevent nucleophilic attack of the function by the ferrocenyllithium formed. The expected iodoferrocene derivatives were obtained in most cases although the presence of electron-acceptor substituents on the aryl moiety was found to reroute the functionalization on this cycle, in agreement with our DFT calculations (pK_a values after coordination to lithium).

The development of an enantioselective version of the reaction was next attempted using a chiral lithium amide. Although our best *ee* did not exceed 60%, the feasibility of this approach was demonstrated. Finally, we took advantage of the installation of the iodine on the (hetero)aryl ring to reach original ferrocene-fused heterocycles, including a tetracycle obtained by enantioselective C–H functionalization.

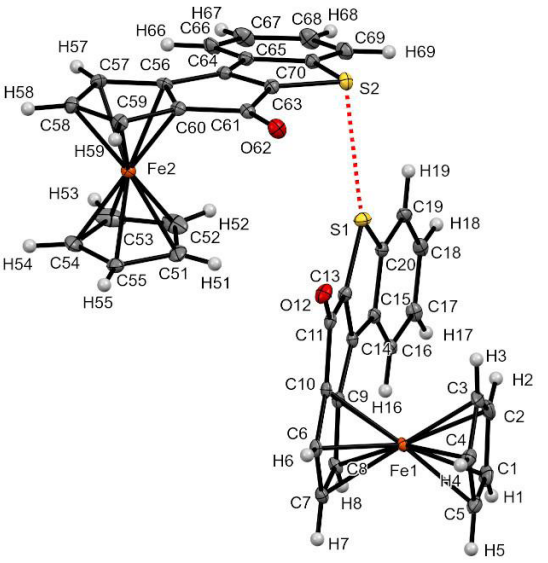

Figure 11. Chalcogen–chalcogen bond observed in the solid state for compound ***R*P-12**. Thermal ellipsoids shown at the 30% probability level. Selected bond lengths (Å) and angles (°): S1···S2 = 3.547, C13–S1···S2 124.90, C20–S1···S2 144.94, C63–S2···S1 105.11, C70–S2···S1 76.54, angle plane (C9–C8–C7–C6–C10–C11–C13–S1–C20–C19–C18–C17–C16–C15–C14)-(C56–C57–C58–C59–C60–C61–C63–S2–C70–C69–C68–C67–C66–C65–C64) 89.24.

Given the significant potential of both ferrocene ketones [65] and ferrocene-fused heterocycles [153], the current study is expected to pave the way for future work toward such compounds to promote their application in various fields.

Acknowledgments

We acknowledge BASF (generous gift of di[(*S*)-1-phenylethyl]amine and di[(*R*)-1-phenylethyl]amine) and Thermofisher (generous gift of 2,2,6,6-tetramethylpiperidine). We acknowledge Olivier Perez, Carmelo Prestipino and Jean-François Lohier (CRISMAT, UMR CNRS 6508) and well as Magali Allain (Moltech-Anjou, UMR CNRS 6200) for their help in X-ray data collection.

Declaration of interests

The authors do not work for, advise, own shares in, or receive funds from any organization that could benefit from this article, and have declared no affiliations other than their research organizations.

Funding

This work was supported by the Direction Générale de la Recherche Scientifique et du Développement Technologique (MH), Rennes Métropole (WE), the University of Carthage and the Tunisian Ministry of Higher Education and Scientific Research (SB), the Fonds Européen de Développement Régional (FEDER; D8 VENTURE Bruker AXS diffractometer), the Université de Rennes and the Centre National de la Recherche Scientifique (WE, J-PH, MB, TR, FM).

Supplementary materials

Supporting information for this article is available on the journal's website under https://doi.org/10.5802/crchim.429 or from the author.

The CCDC files 2490197 (**1-*o*OMePh**), 2490198 (**1-*p*ClPh**), 2490199 (**1-*m*BrPh**), 2490200 (**1-*o*CF$_3$Ph**), 2490201 (**1-*m*CF$_3$Ph**), 2490202 (**1-*p*CF$_3$Ph**), 2490203 (**1-*o*FPh**), 2490204 (**1-2BTh**), 2490205 (**1-C≡CPh**), 2490206 [***R*P-2-Ph**], 2490207 (**2-*o*OMePh**), 2490208 (**2-*p*OMePh**), 2490209 (**2-*o*ClPh**), 2490210 (**2-*p*ClPh**), 2490211 [***R*P-2-*o*BrPh**], 2490212 [***S*P-2-*o*BrPh**], 2490213 (**2-*p*BrPh**), 2490214 (**2-*p*CF$_3$Ph**), 2490215 (**2′-2Py**), 2490216 (**2′-2BTh**), 2490217 (**2″-2BTh**) and 2490218 (**12**) contain the supplementary crystallographic data. These data can be obtained free of charge from the Cambridge Crystallographic Data Center via www.ccdc.cam.ac.uk/structures.

References

[1] T. J. Kealy and P. L. Pauson, "A new type of organo-iron compound", *Nature* **168** (1951), pp. 1039–1040.

[2] S. A. Miller, J. A. Tebboth and J. F. Tremaine, "Dicyclopentadienyliron", *J. Chem. Soc.* **1952** (1952), pp. 632–635.

[3] G. Wilkinson, M. Rosenblum, M. C. Whiting and R. B. Woodward, "The structure of iron biscyclopentadienyl", *J. Am. Chem. Soc.* **74** (1952), pp. 2125–2126.

[4] E. O. Fischer and W. Pfab, "Cyclopentadiene-metallic complex, a new type of organo-metallic compound", *Z. Naturforsch.* **7b** (1952), pp. 377–379.

[5] G. G. A. Balavoine, J. C. Daran, G. Iftime, E. Manoury and C. Moreau-Bossuet, "Selective synthesis of ferrocenes", *J. Organomet. Chem.* **567** (1998), pp. 191–198.

[6] C. J. Richards and A. J. Locke, "Recent advances in the generation of non-racemic ferrocene derivatives and their application to asymmetric synthesis", *Tetrahedron Asymmetry* **9** (1998), pp. 2377–2407.

[7] R. C. J. Atkinson, V. C. Gibson and N. J. Long, "The syntheses and catalytic applications of unsymmetrical ferrocene ligands", *Chem. Soc. Rev.* **33** (2004), pp. 313–328.

[8] I. R. Butler, "The simple synthesis of ferrocene ligands from a practitioner's perspective", *Eur. J. Inorg. Chem.* **15** (2012), pp. 4387–4406.

[9] F. A. Larik, A. Saeed, T. A. Fattah, U. Muqadar and P. A. Channar, "Recent advances in the synthesis, biological activities and various applications of ferrocene derivatives", *Appl. Organomet. Chem.* **31** (2017), article no. e3664.

[10] D. Astruc, "The numerous paths of ferrocene", *Nat. Chem.* **15** (2023), p. 1650.

[11] A. Straube, L. Useini and E. Hey-Hawkins, "Multiferrocene-based ligands: From design to applications", *Chem. Rev.* **125** (2025), pp. 3007–3058.

[12] H. Qi, N.-N. Hang and J. Ming, "Synthesis of planar chiral ferrocenes by catalytic desymmetrization reactions", *ChemCatChem* **16** (2024), article no. e202400736.

[13] S. E. Park, S. Park, W. Lee and J. M. Joo, "Recent strategies for the synthesis of ferrocene derivatives and their applications to electrochemistry", *Synthesis* **57** (2025), pp. 2411–2422.

[14] T. J. Colacot, "A concise update on the applications of chiral ferrocenyl phosphines in homogeneous catalysis leading to organic synthesis", *Chem. Rev.* **103** (2003), pp. 3101–3118.

[15] R. Gómez-Arrayás, J. Adrio and J. C. Carretero, "Recent applications of chiral ferrocene ligands in asymmetric catalysis", *Angew. Chem. Int. Ed.* **45** (2006), pp. 7674–7715.

[16] In, *Chiral Ferrocenes in Asymmetric Catalysis: Synthesis and Applications*, Wiley-VCH: Weinheim, 2010.

[17] K. Yoshida and R. Yasue, "Planar-chiral ferrocene-based N-heterocyclic carbene ligands", *Chem. Eur. J.* **24** (2018), pp. 18575–18586.

[18] In, *Ferrocenes: Ligands, Materials and Biomolecules*, Wiley: Chichester, 2008.

[19] G. Roy, R. Gupta, S. Ranjan Sahoo, S. Saha, D. Asthana and P. Chandra Mondal, "Ferrocene as an iconic redox marker: From solution chemistry to molecular electronic devices", *Coord. Chem. Rev.* **473** (2022), article no. 214816.

[20] S. K. Sahoo, "Fluorescent chemosensors containing redox-active ferrocene: a review", *Dalton Trans.* **50** (2021), pp. 11681–11700.

[21] A. A. J. Torriero, A. M. Torriero, K. T. Miller and A. K. V. Mruthunjaya, "Beyond cations: Expanding the horizons of ferrocene-based electrochemical sensors for neutral and anionic molecules", *Inorganics* **13** (2025), article no. 3.

[22] D. R. van Staveren and N. Metzler-Nolte, "Bioorganometallic chemistry of ferrocene", *Chem. Rev.* **104** (2004), pp. 5931–5985.

[23] M. Patra and G. Gasser, "The medicinal chemistry of ferrocene and its derivatives", *Nat. Rev. Chem.* **1** (2017), article no. 0066.

[24] B. Sharma and V. Kumar, "Has ferrocene really delivered its role in accentuating the bioactivity of organic scaffolds?", *J. Med. Chem.* **64** (2021), pp. 16865–16921.

[25] V. Tomar, P. Kumar, D. Sharma, R. K. Joshi and M. Nemiwal, "Anticancer potential of ferrocene-containing derivatives: Current and future prospective", *J. Mol. Struct.* **1319** (2025), article no. 139589.

[26] L. Ezell, D. H. LaVoy, T. Sasaki and L. M. Goldman, "Solvent-free acylation of ferrocene: Crowdsourcing student data to evaluate reaction conditions", *J. Chem. Educ.* **102** (2025), pp. 2422–2428.

[27] F. Rebière, O. Samuel and H. B. Kagan, "A convenient method for the preparation of monolithioferrocene", *Tetrahedron Lett.* **31** (1990), pp. 3121–3124.

[28] R. Sanders and U. T. Mueller-Westerhoff, "The lithiation of ferrocene and ruthenocene: a retraction and an improvement", *J. Organomet. Chem.* **512** (1996), pp. 219–224.

[29] D. Astruc, "Why is ferrocene so exceptional?", *Eur. J. Inorg. Chem.* **20** (2017), pp. 6–29.

[30] E. Lerayer, L. Radal, T. A. Nguyen, et al., "Highly functionalized ferrocenes", *Eur. J. Inorg. Chem.* **23** (2020), pp. 419–445.

[31] P. Štepnička, "Forever young: the first seventy years of ferrocene", *Dalton Trans.* **51** (2022), pp. 8085–8102.

[32] M. Korb and H. Lang, "Rearrangements and migrations along the ferrocene periphery: On the way to planar-chiral and (multi)substitution patterns", *Eur. J. Inorg. Chem.* **25** (2022), article no. e202100946.

[33] C. Guchhait, V. Suriyaa, N. Sahu, S. D. Sarkar and B. Adhikari, "Ferrocene: an exotic building block for supramolecular assemblies", *Chem. Commun.* **59** (2023), pp. 14482–14496.

[34] W. Erb and F. Mongin, "Twofold ferrocene C–H lithiations for one-step difunctionalizations", *Synthesis* **51** (2019), pp. 146–160.

[35] B. Ferber and H. B. Kagan, "Metallocene sulfoxides as precursors of metallocenes with planar chirality", *Adv. Synth. Catal.* **349** (2007), pp. 493–507.

[36] V. Mamane, "The diastereoselective ortho-lithiation of Kagan's ferrocenyl acetal. Generation and reactivity of chiral 2-substituted ferrocenecarboxaldehydes", *Tetrahedron Asymmetry* **21** (2010), pp. 1019–1029.

[37] D. Schaarschmidt and H. Lang, "Selective syntheses of planar-chiral ferrocenes", *Organometallics* **32** (2013), pp. 5668–5704.

[38] C.-X. Liu, Q. Gu and S.-L. You, "Asymmetric C–H bond functionalization of ferrocenes: New opportunities and challenges", *Trends Chem.* **2** (2020), pp. 737–749.

[39] W. Erb, M. Wen, T. Roisnel and F. Mongin, "Synthesis of ferrocenesulfonyl chloride, key intermediate toward ferrocenesulfonamides", *Synthesis* **53** (2021), pp. 2612–2620.

[40] W. Erb and T. Roisnel, "The chemistry of ferrocenesulfonyl fluoride revealed", *Dalton Trans.* **50** (2021), pp. 16483–16487.

[41] R. B. Woodward, M. Rosenblum and M. C. Whiting, "A new aromatic system", *J. Am. Chem. Soc.* **74** (1952), pp. 3458–3459.

[42] D. Enders, R. Peters, R. Lochtman and J. Runsink, "Enantioselective synthesis of planar chiral ortho-functionalized ferrocenyl ketones", *Eur. J. Org. Chem.* **3** (2000), pp. 2839–2850.

[43] B. Ferber, S. Top, P. Herson and G. Jaouen, "New ortho-directing group for lithiation: Use of a methoxy-imino auxiliary for the synthesis of chiral ortho-substituted acetyl- and propionylferrocenes", *Organometallics* **26** (2007), pp. 1686–1691.

[44] D. Enders, E. A. Jonas and T. Klumpen, "Efficient asymmetric synthesis of planar-chiral bisferrocenes", *Eur. J. Org. Chem.* **12** (2009), pp. 2149–2162.

[45] E. Hevia, A. R. Kennedy and M. D. McCall, "Assessing the reactivity of sodium zincate [(TMEDA)Na(TMP)Zn^{t}Bu$_2$] towards benzoylferrocene: deprotonative metalation vs. alkylation reactions", *Dalton Trans.* **41** (2012), pp. 98–103.

[46] G. Dayaker, A. Sreeshailam, F. Chevallier, T. Roisnel, P. Radha Krishna and F. Mongin, "Deprotonative metallation of ferrocenes using mixed lithium-zinc and lithium-cadmium combinations", *Chem. Commun.* **46** (2010), pp. 2862–2864.

[47] N. Mokhtari Brikci-Nigassa, G. Bentabed-Ababsa, W. Erb and F. Mongin, "In situ 'trans-metal trapping': An efficient way to extend the scope of aromatic deprotometalation", *Synthesis* **50** (2018), pp. 3615–3633.

[48] C. Bastien, W. Erb, Y. S. Halauko, V. E. Matulis, T. Roisnel, Y. Sarazin and F. Mongin, "Functionalisation of chromane by deprotonative metallation", *Eur. J. Org. Chem.* **27** (2024), article no. e202400566.

[49] M. C. Whisler, S. MacNeil, V. Snieckus and P. Beak, "Beyond thermodynamic acidity: A perspective on the complex-induced proximity effect (CIPE) in deprotonation reactions", *Angew. Chem. Int. Ed.* **43** (2004), pp. 2206–2225.

[50] P. Beak and A. I. Meyers, "Stereo- and regiocontrol by complex induced proximity effects: reactions of organolithium compounds", *Acc. Chem. Res.* **19** (1986), pp. 356–363.

[51] N. J. R. van Eikema Hommes and P. v. R. Schleyer, "Mechanisms of aromatic lithiation. Influence of aggregation and directing groups", *Tetrahedron* **50** (1994), pp. 5903–5916.

[52] A. Abbotto, S. S.-W. Leung, A. Streitwieser and K. V. Kilway, "The role of monomer in alkylation reactions of the lithium enolate of p-phenylisobutyrophenone in tetrahydrofuran", *J. Am. Chem. Soc.* **120** (1998), pp. 10807–10813.

[53] In, *Organometallics in Synthesis: A Manual*, John Wiley & Sons: New York, 1994.

[54] M. Schlosser, "The 2 ∗ 3 toolbox of organometallic methods for regiochemically exhaustive functionalization", *Angew. Chem. Int. Ed.* **44** (2005), pp. 376–393.

[55] R. Maggi and M. Schlosser, "Rate enhancing and rate retarding effects of methoxy substituents on arene metalation", *Tetrahedron Lett.* **40** (1999), pp. 8797–8800.

[56] M. Schlosser, F. Mongin, J. Porwisiak, W. Dmowski, H. H. Buker and N. M. M. Nibbering, "Bis- and oligo(trifluoromethyl)benzenes: Hydrogen/metal exchange rates and gas-phase acidities", *Chem. Eur. J.* **4** (1998), pp. 1281–1286.

[57] D. A. Evans, V. J. Cee, T. E. Smith and K. J. Santiago, "Selective lithiation of 2-methyloxazoles. Applications to pivotal bond constructions in the phorboxazole nucleus", *Org. Lett.* **1** (1999), pp. 87–90.

[58] N. Sharma, J. S. Dhau, A. Singh, S. Abbat, P. V. Bharatam, A. K. Malik and A. Singh, "Selective lithiation of 2,4-lutidine: Role of transition states of lithium dialkylamides", *J. Organomet. Chem.* **936** (2021), article no. 121691.

[59] M. Hasyeoui, P. M. Chapple, F. Lassagne, T. Roisnel, M. Cordier, A. Samarat, Y. Sarazin and F. Mongin, "Lateral deprotometallation-trapping reactions on methylated pyridines, quinolines and quinoxalines using lithium diethylamide", *Eur. J. Org. Chem.* **26** (2023), article no. e202300555.

[60] V. E. Matulis, Y. S. Halauko, O. A. Ivashkevich and P. N. Gaponik, "CH acidity of five-membered nitrogen-containing heterocycles: DFT investigation", *J. Mol. Struct.: Theochem* **909** (2009), pp. 19–24.

[61] R. R. Kadiyala, D. Tilly, E. Nagaradja, et al., "Computed CH acidity of biaryl compounds and their deprotonative metalation by using a mixed lithium/Zinc-TMP base", *Chem. Eur. J.* **19** (2013), pp. 7944–7960.

[62] M. Hedidi, W. Erb, F. Lassagne, et al., "Functionalization of pyridyl ketones using deprotolithiation-in situ zincation", *RSC Adv.* **6** (2016), pp. 63185–63189.

[63] M. Hedidi, J. Maillard, W. Erb, et al., "Fused systems based on 2-aminopyrimidines: Synthesis combining deprotolithiation-in situ zincation with N-arylation reactions and biological properties", *Eur. J. Org. Chem.* **20** (2017), pp. 5903–5915.

[64] A. C. Bényei, C. Glidewell, P. Lightfoot, B. J. L. Royles and D. M. Smith, "Functionalized acyl ferrocenes: crystal and molecular structures of 4-aminobenzoylferrocene, 4-hydroxybenzoylferrocene and 1,1'-bis(4-hydroxybenzoyl)ferrocene", *J. Organomet. Chem.* **539** (1997), pp. 177–186.

[65] E. A. Hillard, P. Pigeon, A. Vessières, C. Amatore and G. Jaouen, "The influence of phenolic hydroxy substitution on the electron transfer and anti-cancer properties of compounds based on the 2-ferrocenyl-1-phenyl-but-1-ene motif", *Dalton Trans.* **36** (2007), pp. 5073–5081.

[66] D. Plazuk and J. Zakrzewski, "Friedel-Crafts acylation of ferrocene with alkynoic acids", *J. Organomet. Chem.* **694** (2009), pp. 1802–1806.

[67] P. Švec, O. V. Petrov, J. Lang, et al., "Fluorinated ferrocene moieties as a platform for redox-responsive polymer 19F MRI theranostics", *Macromolecules* **55** (2022), pp. 658–671.

[68] S. Masi, S. Top, L. Boubekeur, G. Jaouen, S. Mundwiler, B. Spingler and R. Alberto, "Direct synthesis of tricarbonyl(cyclopentadienyl)rhenium and tricarbonyl(cyclopentadienyl)technetium units from ferrocenyl moieties - Preparation of 17α-ethynylestradiol derivatives bearing a tricarbonyl(cyclopentadienyl)technetium group", *Eur. J. Inorg. Chem.* **7** (2004), pp. 2013–2017.

[69] A. Seggio, M.-I. Lannou, F. Chevallier, D. Nobuto, M. Uchiyama, S. Golhen, T. Roisnel and F. Mongin, "Ligand-activated lithium-mediated zincation of n-phenylpyrrole", *Chem. Eur. J.* **13** (2007), pp. 9982–9989.

[70] E. Negishi, A. O. King and N. Okukado, "Selective carbon-carbon bond formation via transition metal catalysis. 3.

A highly selective synthesis of unsymmetrical biaryls and diarylmethanes by the nickel- or palladium-catalyzed reaction of aryl- and benzylzinc derivatives with aryl halides", *J. Org. Chem.* **42** (1977), pp. 1821–1823.

[71] E. Negishi, "Palladium- or nickel-catalyzed cross coupling. A new selective method for carbon-carbon bond formation", *Acc. Chem. Res.* **15** (1982), pp. 340–348.

[72] D. R. Gauthier Jr, R. H. Szumigala Jr, P. G. Dormer, J. D. Armstrong III, R. P. Volante and P. J. Reider, "Synthesis of 5-pyridyl-2-furaldehydes via palladium-catalyzed cross-coupling with triorganozincates", *Org. Lett.* **4** (2002), pp. 375–378.

[73] G. Mloston, R. Hamera and H. Heimgartner, "Synthesis of ferrocenyl thioketones and their reactions with diphenyldiazomethane", *Phosph. Sulfur Silicon Relat. Elem.* **190** (2015), pp. 2125–2133.

[74] G. Dayaker, W. Erb, M. Hedidi, et al., "Enantioselective deprotometalation of alkyl ferrocenecarboxylates using bimetallic bases", *New J. Chem.* **45** (2021), pp. 22579–22590.

[75] F. Mongin, "Long-range effect of bromine in the deprotonative metalation of aromatic compounds", *Chimia* **70** (2016), pp. 48–52.

[76] F. Mongin, C. Curty, E. Marzi, F. R. Leroux and M. Schlosser, "Substituent effects on the relative rates and free energies of ortho-lithiation reactions: families of fluorobenzenes as the substrates", *ARKIVOC* **2015** (2015), pp. 48–65.

[77] E. Castagnetti and M. Schlosser, "The trifluoromethoxy group: - a long-range electron-withdrawing substituent", *Chem. Eur. J.* **8** (2002), pp. 799–804.

[78] T. Čarný and R. Šebesta, "Comparison of diastereoselective ortho-metalations and C–H activations of chiral ferrocenes", *Synlett* **35** (2024), pp. 165–182.

[79] Y. Nishibayashi, Y. Arikawa, K. Ohe and S. Uemura, "Enantioselective ortho-lithiation of substituted ferrocenes", *J. Org. Chem.* **61** (1996), pp. 1172–1174.

[80] P. Steffen, C. Unkelbach, M. Christmann, W. Hiller and C. Strohmann, "Catalytic and stereoselective ortholithiation of a ferrocene derivative", *Angew. Chem. Int. Ed.* **52** (2013), pp. 9836–9840.

[81] C. Metallinos, J. Zaifman and L. Dodge, "Aminoferrocene lithiation by boron trifluoride activation", *Org. Lett.* **10** (2008), pp. 3527–3530.

[82] C. Metallinos, J. Zaifman, T. Dudding, L. Van Belle and K. Taban, "Asymmetric lithiation of boron trifluoride-activated aminoferrocenes: An experimental and computational investigation", *Adv. Synth. Catal.* **352** (2010), pp. 1967–1982.

[83] M. Tsukazaki, M. Tinkl, A. Roglans, B. J. Chapell, N. J. Taylor and V. Snieckus, "Direct and highly enantioselective synthesis of ferrocenes with planar chirality by (-)-sparteine-mediated lithiation", *J. Am. Chem. Soc.* **118** (1996), pp. 685–686.

[84] C. Metallinos, H. Szillat, N. J. Taylor and V. Snieckus, "(-)-Sparteine-mediated directed ortho-metalation of N-cumyl-N-ethylferrocenecarboxamide. Versatile routes to functionalized planar chiral ferrocenecarboxamides, amines, esters and phosphines", *Adv. Synth. Catal.* **345** (2003), pp. 370–382.

[85] C. Genet, S. J. Canipa, P. O'Brien and S. Taylor, "Catalytic asymmetric synthesis of ferrocenes and P-stereogenic bisphosphines", *J. Am. Chem. Soc.* **128** (2006), pp. 9336–9337.

[86] W. Erb, T. Roisnel and V. Dorcet, "Practical chromatography-free synthesis of 2-iodo-N,N-diisopropylferrocenecarboxamide and further transformations", *Synthesis* **51** (2019), pp. 3205–3213.

[87] M. Wen, W. Erb, F. Mongin, et al., "Enantioselective synthesis of planar chiral ferrocene triflones", *Adv. Synth. Catal.* **366** (2024), pp. 4984–4993.

[88] D. Price and N. S. Simpkins, "Concerning the asymmetric metalation of ferrocenes by chiral lithium amide bases", *Tetrahedron Lett.* **36** (1995), pp. 6135–6136.

[89] M. Hedidi, G. Dayaker, Y. Kitazawa, et al., "Enantioselective deprotometalation of N,N-dialkyl ferrocenecarboxamides using metal amides", *New J. Chem.* **43** (2019), pp. 14898–14907.

[90] G. Dayaker, D. Tilly, F. Chevallier, G. Hilmersson, P. C. Gros and F. Mongin, "Enantioselective metalation of N,N-diisopropylferrocenecarboxamide and methyl ferrocenecarboxylate using lithium-metal chiral bases", *Eur. J. Org. Chem.* **2012** (2012), pp. 6051–6057.

[91] N. M. Brikci-Nigassa, G. Bentabed-Ababsa, W. Erb and F. Mongin, "In situ 'trans-metal trapping': An efficient way to extend the scope of aromatic deprotometalation", *Synthesis* **50** (2018), pp. 3615–3633.

[92] W. Erb, M. Wen, J.-P. Hurvois, F. Mongin, Y. S. Halauko, O. A. Ivashkevich, V. E. Matulis and T. Roisnel, "*O*-isopropylferrocenesulfonate: Synthesis of polysubstituted derivatives and electrochemical study", *Eur. J. Inorg. Chem.* **24** (2021), pp. 3165–3176.

[93] S. Monticelli, L. Castoldi, I. Murgia, et al., "Recent advancements on the use of 2-methyltetrahydrofuran in organometallic chemistry", *Monatsh. Chem.* **148** (2017), pp. 37–48.

[94] D. Marquarding, H. Klusacek, G. Gokel, P. Hoffmann and I. Ugi, "Stereoselective syntheses. VI. Correlation of central and planar chirality in ferrocene derivatives", *J. Am. Chem. Soc.* **92** (1970), pp. 5389–5393.

[95] L. F. Battelle, R. Bau, G. W. Gokel, R. T. Oyakawa and I. K. Ugi, "Stereoselective synthesis. VIII. Absolute configuration of a 1,2-disubstituted ferrocene derivative with planar and central elements of chirality and the mechanism of the optically active α-ferrocenyl tertiary amines", *J. Am. Chem. Soc.* **95** (1973), pp. 482–486.

[96] G. A. Olah, A.-h. Wu and O. Farooq, "Synthetic methods and reactions. 168. Ring tert-butylation of benzophenones and benzaldehyde with tert-butyllithium and thionyl chloride", *Synthesis* **23** (1991), pp. 1179–1182.

[97] H. Yamataka, Y. Kawafuji, K. Nagareda, N. Miyano and T. Hanafusa, "Electron transfer in the additions of organolithium reagents to benzophenone and benzaldehyde", *J. Org. Chem.* **54** (1989), pp. 4706–4708.

[98] E. Hevia, G. W. Honeyman, A. R. Kennedy and R. E. Mulvey, "Trapping, stabilization, and characterization of an enolate anion of a 1,6-adduct of benzophenone chelated

by a sodium alkylamidozincate cation", *J. Am. Chem. Soc.* **127** (2005), pp. 13106–13107.

[99] D. R. Armstrong, J. A. Garden, A. R. Kennedy, R. E. Mulvey and S. D. Robertson, "Modifying alkylzinc reactivity with 2,2′-dipyridylamide: Activation of tBu–Zn bonds for para-alkylation of benzophenone", *Angew. Chem. Int. Ed.* **52** (2013), pp. 7190–7193.

[100] D. R. Armstrong, E. V. Brouillet, A. R. Kennedy, J. A. Garden, M. Granitzka, R. E. Mulvey and J. J. Trivett, "Donor-activated alkali metal dipyridylamides: co-complexation reactions with zinc alkyls and reactivity studies with benzophenone", *Dalton Trans.* **43** (2014), pp. 14409–14423.

[101] J. J. Crawford, B. J. Fleming, A. R. Kennedy, J. Klett, C. T. O'Hara and S. A. Orr, "Remote functionalization via sodium alkylamidozincate intermediates: access to unusual fluorenone and pyridyl ketone reactivity patterns", *Chem. Commun.* **47** (2011), pp. 3772–3774.

[102] D. R. Armstrong, L. Balloch, J. J. Crawford, et al., "Single electron transfer (SET) activity of the dialkyl-amido sodium zincate [(TMEDA)·Na(μ-TMP)(μ-tBu)Zn(tBu)] towards TEMPO and chalcone", *Chem. Commun.* **48** (2012), pp. 1541–1543.

[103] N. Miyaura, K. Yamada and A. Suzuki, "A new stereospecific cross-coupling by the palladium-catalyzed reaction of 1-alkenylboranes with 1-alkenyl or 1-alkynyl halides", *Tetrahedron Lett.* **20** (1979), pp. 3437–3440.

[104] N. Miyaura and A. Suzuki, "Palladium-catalyzed cross-coupling reactions of organoboron compounds", *Chem. Rev.* **95** (1995), pp. 2457–2483.

[105] M. Tazi, W. Erb, Y. S. Halauko, O. A. Ivashkevich, V. E. Matulis, T. Roisnel, V. Dorcet and F. Mongin, "From 2- to 3-substituted ferrocene carboxamides or how to apply halogen "dance" to the ferrocene series", *Organometallics* **36** (2017), pp. 4770–4778.

[106] W. Erb, L. Kadari, K. Al-Mekhlafi, T. Roisnel, V. Dorcet, P. Radha Krishna and F. Mongin, "Functionalization of 3-iodo-N,N-diisopropylferrocene-carboxamide, a pivotal substrate to open the chemical space to 1,3-disubstituted ferrocenes", *Adv. Synth. Catal.* **362** (2020), pp. 832–850.

[107] S. W. Wright, D. L. Hageman and L. D. McClure, "Fluoride-mediated boronic acid coupling reactions", *J. Org. Chem.* **59** (1994), pp. 6095–6097.

[108] T. E. Barder, S. D. Walker, J. R. Martinelli and S. L. Buchwald, "Catalysts for Suzuki–Miyaura coupling processes: Scope and studies of the effect of ligand structure", *J. Am. Chem. Soc.* **127** (2005), pp. 4685–4696.

[109] K. Sonogashira, Y. Tohda and N. Hagihara, "Convenient synthesis of acetylenes. Catalytic substitutions of acetylenic hydrogen with bromo alkenes, iodo arenes, and bromopyridines", *Tetrahedron Lett.* **16** (1975), pp. 4467–4470.

[110] M. S. Inkpen, A. J. P. White, T. Albrecht and N. J. Long, "Rapid Sonogashira cross-coupling of iodoferrocenes and the unexpected cyclo-oligomerization of 4-ethynylphenylthioacetate", *Chem. Commun.* **49** (2013), pp. 5663–5665.

[111] N. Kausch-Busies, J. M. Neudörfl, P. Wefelmeier, A. Prokop, H. Kühn and H.-G. Schmalz, "Stereoselective synthesis and biological evaluation of ferrocene-containing 5-hydroxyeicosatetraenoic acid analogues", *Eur. J. Org. Chem.* **2011** (2011), pp. 4634–4644.

[112] K. Yoshida, Q. Liu, R. Yasue, S. Wada, R. Kimura, T. Konishi and M. Ogasawara, "Versatile and enantioselective preparation of planar-chiral metallocene-fused 4-dialkylaminopyridines and their application in asymmetric organocatalysis", *ACS Catal.* **10** (2020), pp. 292–301.

[113] C. Duro, T. Jernei, K. J. Szekeres, et al., "Synthesis and SAR analysis of novel 4-hydroxytamoxifen analogues based on their cytotoxic activity and electron-donor character", *Molecules* **27** (2022), article no. 6758.

[114] O. Bernardo, S. González-Pelayo and L. A. López, "Synthesis and applications of ferrocene-fused nitrogen heterocycles", *Eur. J. Inorg. Chem.* **2022** (2022), article no. e202100911.

[115] S. Sangeetha, P. Muthupandi and G. Sekar, "Copper-catalyzed domino synthesis of 2-arylthiochromanones through concomitant C–S bond formations using xanthate as sulfur source", *Org. Lett.* **17** (2015), pp. 6006–6009.

[116] J. Wang, Z.-H. Zhu, M.-W. Chen, Q.-A. Chen and Y.-G. Zhou, "Catalytic biomimetic asymmetric reduction of alkenes and imines enabled by chiral and regenerable NAD(P)H models", *Angew. Chem. Int. Ed.* **58** (2019), pp. 1813–1817.

[117] D.-W. Gao, C. Zheng, Q. Gu and S.-L. You, "Pd-Catalyzed highly enantioselective synthesis of planar chiral ferrocenylpyridine derivatives", *Organometallics* **34** (2015), pp. 4618–4625.

[118] M. C. Whiting, "Recollections of the arrival of ferrocene", *J. Organomet. Chem.* **637–639** (2001), pp. 16–17.

[119] M. Rosenblum, "The early ferrocene days-a personal recollection", *J. Organomet. Chem.* **637–639** (2001), pp. 13–15.

[120] Y. Yamaguchi, W. Ding, C. T. Sanderson, M. L. Borden, M. J. Morgan and C. Kutal, "Electronic structure, spectroscopy, and photochemistry of group 8 metallocenes", *Coord. Chem. Rev.* **251** (2007), pp. 515–524.

[121] J. Jia, Y. Cui, L. Han, W. Sheng, Y. Li and J. Gao, "Syntheses, third-order optical nonlinearity and DFT studies on benzoylferrocene derivatives", *Dyes Pigm.* **104** (2014), pp. 137–145.

[122] W. F. Little, C. N. Reilley, J. D. Johnson and A. P. Sanders, "Chronopotentiometric studies of ferrocene derivatives. II. Directly substituted ferrocenes", *J. Am. Chem. Soc.* **86** (1964), pp. 1382–1386.

[123] W. E. Britton, R. Kashyap, M. El-Hashash, M. El-Kady and M. Herberhold, "The anomalous electrochemistry of the ferrocenylamines", *Organometallics* **5** (1986), pp. 1029–1031.

[124] D. A. Khobragade, S. G. Mahamulkar, L. Pospíšil, I. Císařová, L. Rulíšek and U. Jahn, "Acceptor-substituted ferrocenium salts as strong, single-electron oxidants: Synthesis, electrochemistry, theoretical investigations, and initial synthetic application", *Chem. Eur. J.* **18** (2012), pp. 12267–12277.

[125] G. L. K. Hoh, W. E. McEwen and J. Kleinberg, "Substituent effects in the chronopotentiometric oxidation of ferrocenes", *J. Am. Chem. Soc.* **83** (1961), pp. 3949–3953.

[126] C. Saboureau, M. Troupel, S. Sibille and J. Perichon, "Electroreductive coupling of trifluoromethylarenes with electrophiles: synthetic applications", *J. Chem. Soc. Chem. Commun.* **25** (1989), pp. 1138–1139.

[127] C. P. Andrieux, C. Combellas, F. Kanoufi, J.-M. Savéant and A. Thiebault, "Dynamics of bond breaking in ion radicals. Mechanisms and reactivity in the reductive cleavage of carbon-fluorine bonds of fluoromethylarenes", *J. Am. Chem. Soc.* **119** (1997), pp. 9527–9540.

[128] R. I. Pacut and E. Kariv-Miller, "Birch-type reductions in aqueous media. Benzo[b]thiophene and diphenyl ether", *J. Org. Chem.* **51** (1986), pp. 3468–3470.

[129] W. Erb, N. Richy, J.-P. Hurvois, P. J. Low and F. Mongin, "From ferrocene to 1,2,3,4,5-pentafluoroferrocene: halogen effect on the properties of metallocene", *Dalton Trans.* **50** (2021), pp. 16933–16938.

[130] C. Hansch, A. Leo and R. W. Taft, "A survey of Hammett substituent constants and resonance and field parameters", *Chem. Rev.* **91** (1991), pp. 165–195.

[131] M. S. Inkpen, S. Du, M. Hildebrand, A. J. P. White, N. M. Harrison, T. Albrecht and N. J. Long, "The unusual redox properties of fluoroferrocenes revealed through a comprehensive study of the haloferrocenes", *Organometallics* **34** (2015), pp. 5461–5469.

[132] D. M. Evans, D. D. Hughes, P. J. Murphy, P. N. Horton, S. J. Coles, F. F. de Biani, M. Corsini and I. R. Butler, "Synthetic route to 1,1′,2,2′-tetraiodoferrocene that avoids isomerization and the electrochemistry of some tetrahaloferrocenes", *Organometallics* **40** (2021), pp. 2496–2503.

[133] S. D. Waniek, J. Klett, C. Förster and K. Heinze, "Polysubstituted ferrocenes as tunable redox mediators", *Beilstein J. Org. Chem.* **14** (2018), pp. 1004–1015.

[134] W. Erb, J.-P. Hurvois, Y. S. Halauko, V. E. Matulis and T. Roisnel, "Exploring the boundaries of ferrocenesulfonyl fluoride chemistry", *Inorg. Chem. Front.* **9** (2022), pp. 5862–5883.

[135] M. Wen, W. Erb, F. Mongin, et al., "From ferrocene to decasubstituted enantiopure ferrocene-1,1′-disulfoxide derivatives", *Dalton Trans.* **52** (2023), pp. 3725–3737.

[136] G. Cavallo, P. Metrangolo, R. Milani, T. Pilati, A. Priimagi, G. Resnati and G. Terraneo, "The halogen bond", *Chem. Rev.* **116** (2016), pp. 2478–2601.

[137] L. Fotović, N. Bedeković and V. Stilinović, "Evaluation of halogenopyridinium cations as halogen bond donors", *Cryst. Growth Des.* **21** (2021), pp. 6889–6901.

[138] K. Raatikainen, M. Cametti and K. Rissanen, "The subtle balance of weak supramolecular interactions: the hierarchy of halogen and hydrogen bonds in haloanilinium and halopyridinium salts", *Beilstein J. Org. Chem.* **6** (2010), pp. 1–13.

[139] G. Levilain and G. Coquerel, "Pitfalls and rewards of preferential crystallization", *CrystEngComm* **12** (2010), pp. 1983–1992.

[140] M. Wen, W. Erb, F. Mongin, Y. S. Halauko, O. A. Ivashkevich, V. E. Matulis, T. Roisnel and V. Dorcet, "Functionalization of N,N-dialkylferrocenesulfonamides toward substituted derivatives", *Organometallics* **40** (2021), pp. 1129–1147.

[141] M. Wen, W. Erb, F. Mongin, Y. S. Halauko, O. A. Ivashkevich, V. E. Matulis and T. Roisnel, "Synthesis of polysubstituted ferrocenesulfoxides", *Molecules* **27** (2022), article no. 1798.

[142] V. Mamane, P. Peluso, E. Aubert, R. Weiss, E. Wenger, S. Cossu and P. Pale, "Disubstituted ferrocenyl iodo- and chalcogenoalkynes as chiral halogen and chalcogen bond donors", *Organometallics* **39** (2020), pp. 3936–3950.

[143] S. Scheiner, "Characterization of type I and II interactions between halogen atoms", *Cryst. Growth Des.* **22** (2022), pp. 2692–2702.

[144] B. K. Saha, R. V. P. Veluthaparambath and V. Krishna G, "Halogen···halogen interactions: Nature, directionality and applications", *Chem. Asian J.* **18** (2023), article no. e202300067.

[145] T. Moriuchi, "Helical chirality of ferrocene moieties in cyclic ferrocene-peptide conjugates", *Eur. J. Inorg. Chem.* **2022** (2022), article no. e202100902.

[146] M. Fellert, R. Hein, A. Ryabchun, Y. Gisbert, C. N. Stindt and B. L. Feringa, "A multiresponsive ferrocene-based chiral overcrowded alkene twisting liquid crystals", *Angew. Chem. Int. Ed.* **64** (2025), article no. e202413047.

[147] Y. Wang, W. Qi, R. Huang, X. Yang, M. Wang, R. Su and Z. He, "Rational design of chiral nanostructures from self-assembly of a ferrocene-modified dipeptide", *J. Am. Chem. Soc.* **137** (2015), pp. 7869–7880.

[148] H. Yamagishi, T. Fukino, D. Hashizume, T. Mori, Y. Inoue, T. Hikima, M. Takata and T. Aida, "Metal-organic nanotube with helical and propeller-chiral motifs composed of a c10-symmetric double-decker nanoring", *J. Am. Chem. Soc.* **137** (2015), pp. 7628–7631.

[149] R. Gleiter, G. Haberhauer, D. B. Werz, F. Rominger and C. Bleiholder, "From noncovalent chalcogen–chalcogen interactions to supramolecular aggregates: Experiments and calculations", *Chem. Rev.* **118** (2018), pp. 2010–2041.

[150] A. S. Lundemba, D. D. Bibelayi, P. A. Wood, J. Pradon and Z. G. Yav, "σ–hole interactions in small-molecule compounds containing divalent sulfur groups R1-S-R2", *Acta Crystallogr.* **B76** (2020), pp. 707–718.

[151] A. Bondi, "van der Waals volumes and radii", *J. Phys. Chem.* **68** (1964), pp. 441–451.

[152] S. Jin, S.-J. Li, X. Ma, J. Su, H. Chen, Y. Lan and Q. Song, "Elemental-sulfur-enabled divergent synthesis of disulfides, diselenides, and polythiophenes from β-CF3-1,3-enynes", *Angew. Chem. Int. Ed.* **60** (2021), pp. 881–888.

[153] L. A. Casper, K. L. Deuter, A. Rehse and R. F. Winter, "Dimerization of 9-phenyl-ferroceno[2,3]indenylmethyl radicals: Electrochemical and spectroelectrochemical studies", *ACS Org. Inorg. Au* **4** (2024), pp. 395–409.